

A STUDY OF SOME LINE METHODS
FOR THE
MEASUREMENT OF IMPEDANCE
AT
ULTRA-HIGH FREQUENCIES

A Dissertation presented in candidature for the degree of
Master of Science of the University of London

by

Eileen E. Mallett

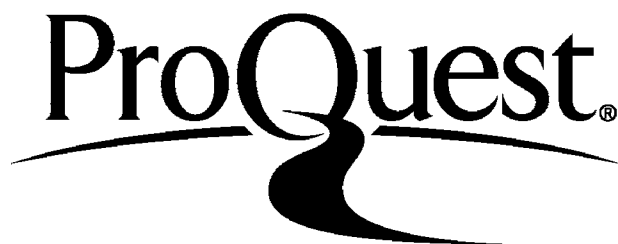
ProQuest Number: 10107205

All rights reserved

INFORMATION TO ALL USERS

The quality of this reproduction is dependent upon the quality of the copy submitted.

In the unlikely event that the author did not send a complete manuscript and there are missing pages, these will be noted. Also, if material had to be removed a note will indicate the deletion.



ProQuest 10107205

Published by ProQuest LLC(2016). Copyright of the Dissertation is held by the Author.

All rights reserved.

This work is protected against unauthorized copying under Title 17, United States Code
Microform Edition © ProQuest LLC.

ProQuest LLC
789 East Eisenhower Parkway
P.O. Box 1346
Ann Arbor, MI 48106-1346

CONTENTS.

Introduction	Page 3.
I An outline of the main methods of measuring impedances at ultra-high frequencies by the use of transmission lines.	Page 5.
II The Current Resonance method for the measurement of impedances	Page 32.
(a) Chipman's method	Page 33.
(b) Essen's experimental study of Chipman's method	Page 38.
III The Double Bridge method for the measurement of impedances	Page 45.
(a) Williams' method	Page 46.
(b) Theoretical and Experimental investigation of Williams' method (Miss) Williamson and (Miss) Harriss)	Page 53.
IV A new method for finding the critical separation of the Double Bridge method	Page 57.
(a) Theory	Page 58.
(b) Experimental Work	Page 60.
V The measurement of an impedance using a system of Lecher wires	Page 66.
(a) Results using the Double Bridge method	Page 68.
(b) Results using the Current Resonance method	Page 70.
(c) Comparison and discussion of results	Page 73.
Conclusion	Page 75.
References	Page 77.

SYMBOLS

- λ Wavelength of electromagnetic wave.
- l Length of line.
- l_0 Resonant length of line
- Δl Width of resonance curve where maximum ordinate is reduced by a factor of two (= $2\delta l$)
- \mathcal{E}_0 Input electro-motive force.
- V_x Voltage at distance x from input end.
- I_x Current at distance x from input end.
- V_y Voltage at distance y from far end.
- I_y Current at distance y from far end.
- Z_x Impedance of lines at distance x from input end.
- Z_0 Terminating impedance at input end.
- Z_r Terminating impedance at far end.
- Z_i Input impedance to line.
- Y_i Input admittance to line.
- Z_0 Characteristic impedance of line.
- Γ Propagation constant of line.
- α Attenuation constant of line.
- β Phase constant of line.
- K_0, K_r Reflection coefficients of Z_0 and Z_r .
- ϕ Phase angle of reflection coefficients.

INTRODUCTION

The standard circuits for the measurement of impedances at frequencies up to about 50 Mc/s are bridge networks although special design incorporating shielding and earthing devices is necessary in the radio-frequency range. The theory of the various bridge methods assumes that the current flowing in any arm of the bridge is constant throughout its path and depends only on the potential difference applied across the arm and the impedance of the arm.

Since the current at any point in a circuit depends on the magnetic field of the electro-magnetic wave in the vicinity and is not constant throughout the whole of its path, this assumption is only permissible for wavelengths which are large compared with the linear dimensions of the apparatus. In fact the current varies from a maximum to a minimum value in a distance $\frac{\lambda}{4}$ where λ is the wavelength of the electro-magnetic wave associated with the current. At a frequency of 100 Mc/s, say $\lambda = 300$ cms and $\frac{\lambda}{4} = 75$ cms. It is impracticable to design bridges of the dimensions of a few centimetres and other methods have to be employed at these higher frequencies.

An outline of these methods is given in Section I followed by a more detailed study of two of the methods in Sections II and III. The difficulty of obtaining a satisfactory short-circuit in order to find the **critical** separation of the

Williams' method was then investigated. This was eliminated by plotting the graphs differently. This work is described in Section IV. Next an impedance was measured on the same apparatus by the Williams method (using this modification) and the Chipman method. These results are described and compared in Section V. Finally in the conclusion it is suggested that the Williams method may prove more useful on a coaxial transmission line than on open Lecher wires.

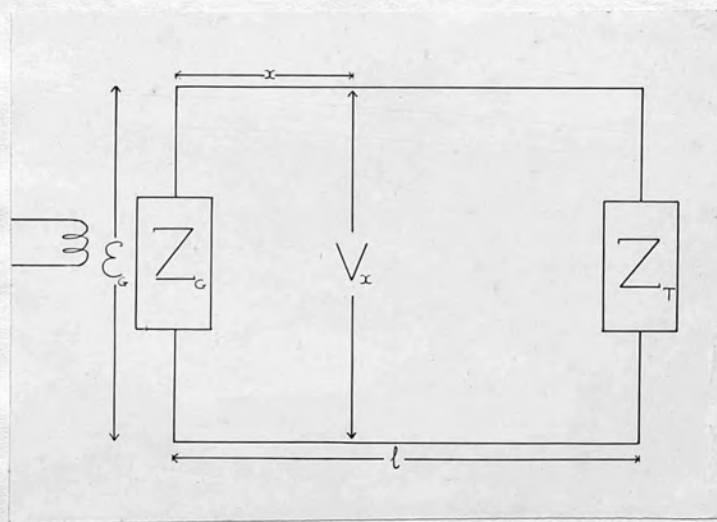
SECTION I

AN OUTLINE OF THE MAIN METHODS OF MEASURING
IMPEDANCES AT ULTRA-HIGH FREQUENCIES BY THE
USE OF TRANSMISSION LINES.

When an alternating electro-motive force is applied to one end of a pair of parallel wires a plane transverse electromagnetic wave is propagated along the line with the same velocity as in free space. Currents are set up in the two conductors and are equal and opposite at any point. The ratio of the potential difference between the wires to the current flowing in them is known as the impedance at that point. If the line is terminated by an impedance the wave is reflected back and a standing-wave pattern consisting of a series of current and voltage nodes and anti-nodes is set up along the line, current nodes coinciding with voltage anti-nodes and vice versa. This leads to various methods of measuring impedances which can be divided into two main types. These will be described in outline with mention of the more important methods. No attempt at chronological order has been made.

The first group of methods may be generally described as resonance methods. The measuring instrument is kept at a fixed position on the line and the length of line varied. Resonance curves of current or voltage are plotted against length of line, first with a shorting-plate at one end and then with the shorting plate replaced by the unknown impedance. The value of the unknown impedance may then be deduced from the change in the resonant length of line and the width of the resonance curves.

Figure (1.1)



For the case of current resonance consider an electro-motive force \mathcal{E}_G injected through an impedance Z_G into a line of length l , the other end of which is terminated in an impedance Z_T (figure 1.1). In the Chipman¹ method of impedance measurement Z_T is the impedance of the current measuring instrument and Z_G the unknown impedance.

The current and voltage at any point on the line can be expressed as the sum of that due to the original transverse electro-magnetic wave and the reflections from both ends. Summation of these shows that the voltage V_x and current I_x at any point distance x from the input end may be expressed as² :-

$$\left. \begin{aligned} V_x &= \frac{\mathcal{E}_G \cdot \frac{Z_0}{Z_0 + Z_G}}{1 - K_G K_T e^{-2Pl}} \left\{ e^{-Px} - (K_T e^{-2Pl}) e^{Px} \right\} \\ I_x &= \frac{\frac{\mathcal{E}_G}{Z_0 + Z_G}}{1 - K_G K_T e^{-2Pl}} \left\{ e^{-Px} + (K_T e^{-2Pl}) e^{Px} \right\} \end{aligned} \right\} (1.1)$$

where Z_0 is the characteristic impedance of the lines and P is the propagation constant of the line (In quoting this equation the signs of K_T and K_G are reversed because in this case they refer to current reflection coefficients as opposed to voltage reflection coefficients in the reference).

P may be written $\alpha + j\beta$ where α is the attenuation constant and β the phase constant of the line.

$$\beta = \frac{2\pi}{\lambda}$$

K_G and K_T are the current reflection coefficients of the impedances Z_G and Z_T .

$$K_G = \frac{Z_0 - Z_G}{Z_0 + Z_G} \quad \text{and} \quad K_T = \frac{Z_0 - Z_T}{Z_0 + Z_T}$$

At the end of the line $x = l$ and by making this substitution in equation (1.1) and putting $2Z_0/(1+K_G)$ for $(Z_0 + Z_G)$, the current \bar{I}_l at the end of the line is given by

$$\bar{I}_l = \frac{E_G(1+K_G)}{2Z_0} \left\{ \frac{e^{-Pl} + K_T e^{-Pl}}{1 - K_G K_T e^{-2Pl}} \right\}$$

This is the current through Z_T and is recorded by the measuring instrument.

$$\bar{I}_l = \frac{E_G(1+K_G)(1+K_T)}{2Z_0} \left\{ \frac{e^{-Pl}}{1 - K_G K_T e^{-2Pl}} \right\}$$

This may be put in the form

$$\bar{I}_l = \bar{I}_0 f(l) \tag{1.2}$$

Where \bar{I}_0 is independent of l and

$$f(l) = \frac{e^{-Pl}}{1 - K_G K_T e^{-2Pl}} \tag{1.3}$$

The product of the two reflection coefficients may be written

$$K_G K_T = e^{-2(P+jq)} \tag{1.4}$$

In which case the phase angle of the product is $-2q$.

Substituting from equation (1.4) in equation (1.3) and writing the propagation constant P in the form $\alpha + j\beta$

$$\begin{aligned}
 f(l) &= \frac{e^{-(\alpha + j\beta)l}}{1 - e^{-2(\rho + jq) - 2(\alpha + j\beta)l}} \\
 &= \frac{1}{e^{(\alpha + j\beta)l} - e^{-2(\rho + jq) - (\alpha + j\beta)l}} \\
 &= \frac{1}{e^{-(\rho + jq)} \{ e^{(\alpha l + \rho) + j(\beta l + q)} - e^{-(\alpha l + \rho) + j(\beta l + q)} \}} \\
 &= \frac{1}{2(K_G K_T)^{\frac{1}{2}} \sinh[(\alpha l + \rho) + j(\beta l + q)]}
 \end{aligned}$$

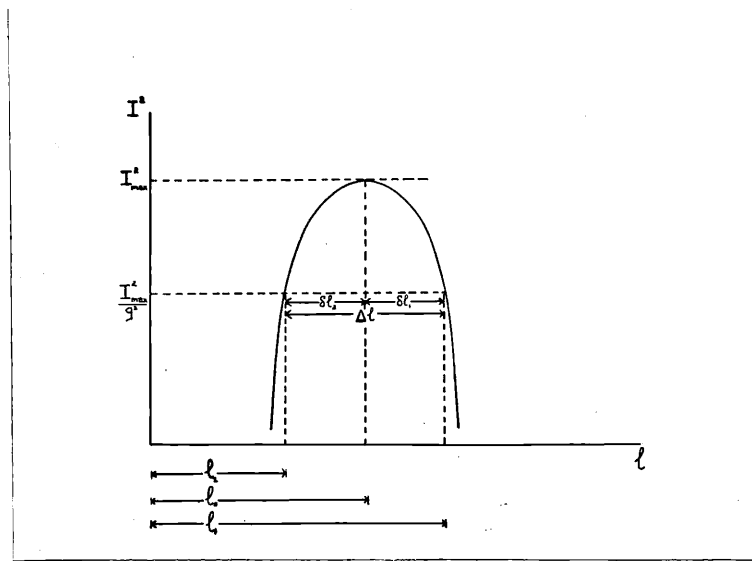
In the Chipman method a thermo-junction is used to measure current so that only the absolute value of $f(l)$ need be considered.

$$\begin{aligned}
 |f(l)|^2 &= \frac{1}{\{2(K_G K_T)^{\frac{1}{2}}\}^2 \cdot \sinh[(\alpha l + \rho) + j(\beta l + q)] \cdot \sinh[(\alpha l + \rho) - j(\beta l + q)]} \\
 |f(l)| &= \frac{1}{2(K_G K_T)^{\frac{1}{2}} [\sinh^2(\alpha l + \rho) + \sin^2(\beta l + q)]^{\frac{1}{2}}} \quad (1.5)
 \end{aligned}$$

If $\alpha \ll \beta$, as is usually the case, the maximum reading of the current meter for varying length of line l occurs when $l = l_0$, say; i.e. when

$$\beta l_0 + q = n\pi \quad (1.6)$$

Figure (1.2)



substituting for β , the value of q is given by

$$q = \frac{2\pi}{\lambda} \left\{ \frac{n\lambda}{2} - l_0 \right\}$$

Thus referring back to equation (1.4) it can be seen that the phase angle ϕ of the product of the reflection coefficients is given by

$$\phi = -2q = \frac{4\pi}{\lambda} \left\{ l_0 - \frac{n\lambda}{2} \right\} \quad (1.7)$$

The maximum value of $|f(l)|$ is given by the substitution of (1.6) in (1.5).

$$|f(l)|_{\max} = \frac{1}{2|K_G K_T|^{\frac{1}{2}} \sinh(\alpha l_0 + p)}$$

The increase in line length, δl_1 , necessary to reduce the current to g times its maximum value (see figure 1.2) is given by

$$\sinh^2[\alpha(l_0 + \delta l_1) + p] + \sin^2 \beta \cdot \delta l_1 = \left\{ \sinh^2(\alpha l_0 + p) \right\} g^2 \quad (1.8)$$

Similarly the decrease in line length δl_2 necessary to reduce the current to this value is given by

$$\sinh^2[\alpha(l_0 - \delta l_2) + p] + \sin^2 \beta \cdot \delta l_2 = \left\{ \sinh^2(\alpha l_0 + p) \right\} g^2 \quad (1.9)$$

Since $\delta l_1 \approx \delta l_2 \approx \delta l$, say, and both are very small compared with l these equations are the same within the limits of experimental measurement and may be written

$$\sinh^2(\alpha l_0 + p) + \sin^2 \frac{2\pi}{\lambda} \cdot \delta l = \left\{ \sinh^2(\alpha l_0 + p) \right\} g^2 \quad (1.10)$$

Thus from a knowledge of the resonant line length l_0 , the half width of the resonance curve δl when the current is reduced from its maximum value by a factor of g , the attenuation constant of the lines α and the wavelength λ , p can be calculated from equation (1.10) and q from equation (1.7). Substitution of these values in equation (1.4) gives the product of the current reflection coefficients $K_G K_T$. Equation (1.4) may be written

$$K_T K_G = |K_T K_G| e^{j\phi_{TG}} \quad (1.11)$$

where ϕ_{TG} is the phase angle of the product of the reflection coefficients.

Since K_T is the reflection coefficient of the impedance of the measuring instrument Z_T , and K_G that of the unknown impedance Z_G , in order to calculate Z_G from K_G ,

K_G must first be extracted from the product $K_G K_T$. This is done by replacing Z_G by a short-circuiting plate or perfect reflector. In this case $K_G = 1$ and the product of the reflection coefficients is of the form

$$|K_T| e^{j\phi_T}$$

where ϕ_T is the phase angle of reflection coefficient of Z_T . Thus the reflection coefficient of the unknown impedance Z_G is given by

$$|K_G| e^{j\phi_G} = \frac{|K_T K_G|}{|K_T|} e^{j(\phi_{TG} - \phi_T)}$$

The phase angle ϕ_G of the reflection coefficient of Z_G is given by substitution from equation (1.7)

$$\phi_G = \phi_{\tau G} - \phi_{\tau} = \frac{4\pi}{\lambda} \left[l_0 - \frac{n\lambda}{2} \right] - \frac{4\pi}{\lambda} \left[l_{s.c.} - \frac{n\lambda}{2} \right]$$

Where $l_{s.c.}$ is the resonant length when Z_G is replaced by a short-circuiting plate

$$\left. \begin{aligned} \phi_G &= \frac{4\pi}{\lambda} [l_0 - l_{s.c.}] \\ \text{and } |K_G| &= \frac{|K_G K_{\tau}|}{|K_{\tau}|} \end{aligned} \right\} (1.12)$$

The resistance and reactance R_G and X_G of the unknown impedance Z_G can be calculated from the current reflection coefficient $K_G = |K_G| e^{j\phi_G}$ as follows.

From the definition of current reflection coefficient

$$K_G = \frac{Z_0 - Z_G}{Z_0 + Z_G}$$

Thus $Z_G = Z_0 \left\{ \frac{1 - K_G}{1 + K_G} \right\}$

Replacing Z_G by $R_G + jX_G$

Z_0 by $R_0 + jX_0$

K_G by $A + jB$

(i.e. $A = |K_G| \cos \phi_G$, $B = |K_G| \sin \phi_G$)

$$R_G + jX_G = (R_0 + jX_0) \left\{ \frac{1 - A - jB}{1 + A + jB} \right\} \quad (1.13)$$

R_G and X_G can be calculated from this equation which can usually be simplified by regarding Z_0 as a pure resistance.

Figure (1.3)

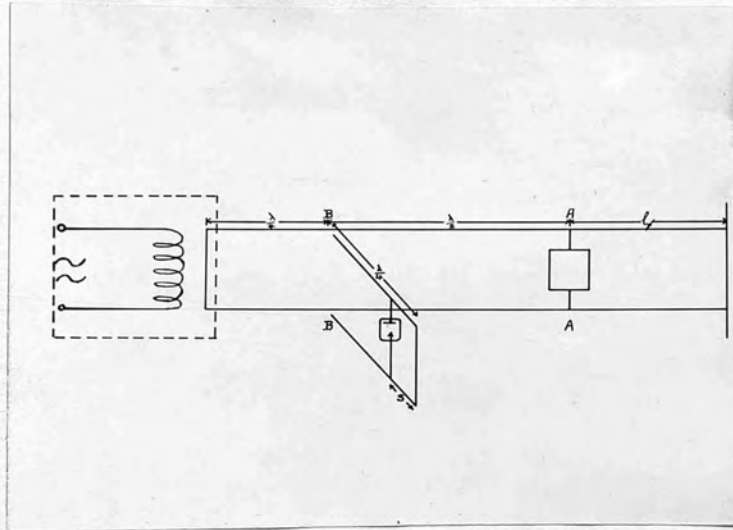
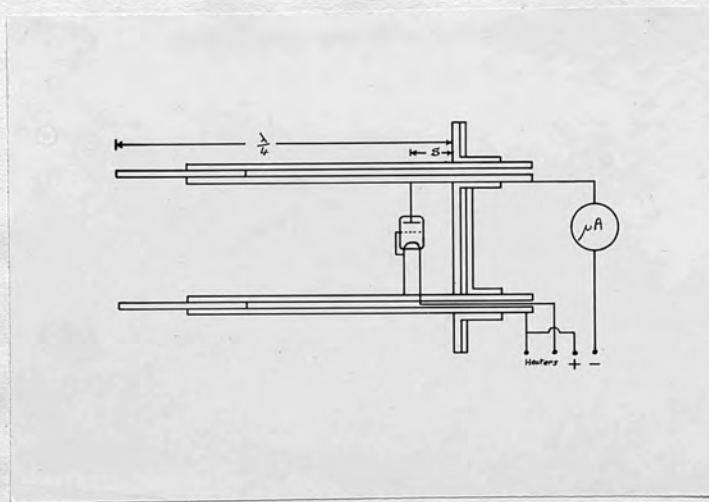


Figure (1.4)



In this latter case

$$\left. \begin{aligned} R_G &= Z_0 \left\{ \frac{1 - A^2 - B^2}{1 + A^2 + B^2 + 2A} \right\} \\ X_G &= \pm Z_0 \left\{ \frac{2B}{1 + A^2 + B^2 + 2A} \right\} \end{aligned} \right\} (1.14)$$

This method as it was used by Chipman and later Essen is described in detail in Section II. The method has the disadvantage that for high values of terminating impedance and for values near the characteristic impedance of the line the resonance curve becomes very flat and the measurements cease to be sufficiently accurate.

Impedance can also be measured on a line by using voltage resonance. The following method employing this principle is due to Kaufmann³. In the apparatus shown in figure (1.3) a shielded oscillator is loosely coupled through a shorting-plate to a Lecher wire system consisting of two parallel brass lines. Measurements are made by a diode voltmeter which is supported at right angles to the lines without actually touching them and is shown in more detail in figure (1.4). The distance S is adjusted to vary the sensitivity of the voltmeter.

Referring back to figure (1.1) the impedance Z_x at any point on the line is given by $\frac{V_x}{I_x}$. Equation (1.1) gives expressions for V_x and I_x where K_G and K_T refer to current reflection coefficients. Since we are now considering voltage resonance it is simpler to use voltage reflection coefficients, the only difference being a change of sign in

each case. Thus

$$\left. \begin{aligned} V_x &= \frac{\frac{E_G Z_0}{Z_0 + Z_G}}{1 - K_G K_T e^{-2Pl}} \left\{ e^{-Px} + (K_T e^{-2Pl}) e^{Px} \right\} \\ I_x &= \frac{\frac{E_G}{Z_0 + Z_G}}{1 - K_G K_T e^{-2Pl}} \left\{ e^{-Px} - (K_T e^{-2Pl}) e^{Px} \right\} \end{aligned} \right\} (1.15)$$

The input impedance Z_i is obtained by putting $x = 0$ in equation (1.15) and substituting in $Z_x = \frac{V_x}{I_x}$

$$Z_i = Z_0 \frac{(1 + K_T e^{-2Pl})}{(1 - K_T e^{-2Pl})} \quad (1.16)$$

The position of the shorting-plate at the end of the line is first adjusted until a system of standing waves can be detected on the line. In this case $K_T = \infty$ in equation (1.16) which becomes

$$Z_i = Z_0 \tanh Pl \quad (1.17)$$

For low-loss lines P can be replaced by $j\beta = j \frac{2\pi}{\lambda}$ so that when $l = \frac{n\lambda}{4}$ where n is any integer

$$Z_i = j Z_0 \tan \frac{n\pi}{2} \quad \text{i.e. } Z_i \rightarrow \infty \quad (1.18)$$

The positions corresponding to these values of l are voltage anti-nodes. The voltmeter is placed at the first anti-node BB, a distance $\frac{\lambda}{4}$ from the input end, and the unknown impedance at the next, AA, $\frac{3\lambda}{4}$ from the input end. Thus the input impedance to the left of AA (or BB) looking towards the generator is very large and variations in the part of the circuit to the right of AA (the measuring circuit) do not affect the input

current. In the theory following AA is taken as the origin of distances measured along the line. Also since the voltage pattern repeats itself with period $\frac{\lambda}{2}$ the voltage measured at BB is the same as that at AA.

The first measurements are made without the unknown impedance connected across the line. The distance l , from AA to the end shorting-plate, is adjusted to give maximum voltage at AA. This is equivalent to maximum input impedance of the line to the right of AA and from equation (1.18) occurs when $l = \frac{\lambda}{4}$. Let this value of $l = l_0$ say.

The unknown impedance Z_T is then put across the lines at AA and l re-adjusted for maximum voltage at AA. Let this value of $l = l_T$ and let G and B be the conductance and susceptance of Z_T .

The input admittance Y_i of the circuit to the right of AA is then given by

$$\begin{aligned} Y_i &= G + jB + \frac{1}{Z_0} \coth \beta l_T \\ &= G + j(B - \frac{1}{Z_0} \cot \beta l_T) \end{aligned}$$

The maximum voltage corresponds to the minimum value of Y_i and the latter occurs where

$$B = \frac{1}{Z_0} \cot \beta l_T \quad (1.19)$$

$$\begin{aligned} \text{Thus } B &= \frac{1}{Z_0} \tan\left(\frac{\pi}{2} - \beta l_T\right) \\ &= \frac{1}{Z_0} \tan \frac{2\pi}{\lambda} (l_0 - l_T) \end{aligned} \quad (1.20)$$

From this equation the susceptance of the unknown impedance

may be found. Z_0 is calculated from the dimensions of the lines and $(l_0 - l_r)$ is measured with a micrometer screw arrangement.

The value of the conductance G of the unknown impedance is obtained by plotting the resonance curve of voltage against length of line l with the unknown impedance Z_r attached to the line. In this case, if the maximum value of the voltage is V_{max} , say, the ratio of V_{max} to any other value of the voltage V is given by

$$\frac{V_{max}}{V} = \frac{G + j(B - \frac{1}{Z_0} \cot \beta l)}{G}$$

substituting for B from equation (1.19)

$$\frac{V_{max}}{V} = \frac{G + \frac{j}{Z_0} (\cot \beta l_r - \cot \beta l)}{G}$$

Since it is only the square of the absolute value of the voltage that is observed it is V_{max}^2 / V^2 that is of interest.

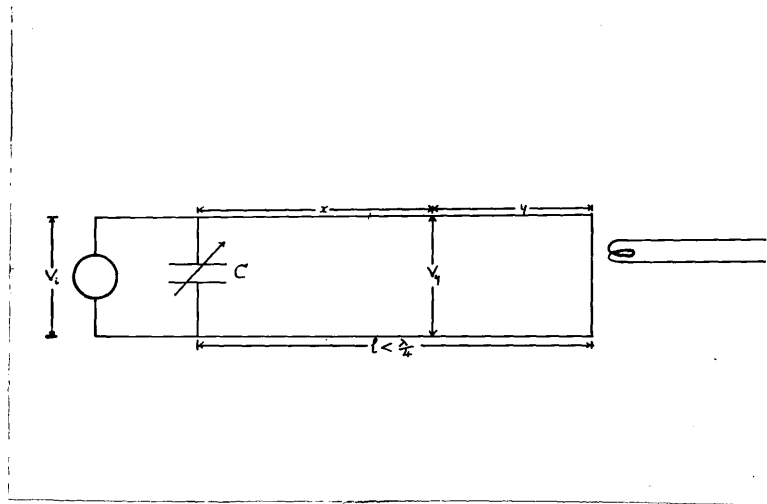
$$\frac{V_{max}^2}{V^2} = g^2 (\text{say}) = \frac{G^2 + \frac{1}{Z_0^2} (\cot \beta l_r - \cot \beta l)^2}{G^2}$$

$$\begin{aligned} \text{Thus } G \sqrt{g^2 - 1} &= \frac{1}{Z_0} (\cot \beta l_r - \cot \beta l) \\ &= \frac{1}{Z_0} [\tan(\frac{\pi}{2} - \beta l_r) - \tan(\frac{\pi}{2} - \beta l)] \\ &= \frac{1}{Z_0} [\tan \frac{2\pi}{\lambda} (l_0 - l_r) - \tan \frac{2\pi}{\lambda} (l_0 - l_r - \frac{\Delta l}{2})] \quad (1.21) \end{aligned}$$

Where Δl is the width of the curve at $V^2 = \frac{V_{max}^2}{g^2}$ (See figure (1.2) which is exactly similar if voltage is substituted for current).

From equation (1.21) the conductance of the unknown

Figure (1.5)



impedance can be found and knowing this and the susceptance, the admittance and impedance can be calculated.

A substitution method for the measurement of admittances at high frequencies has been described by Miller and Salzberg⁴. This is different in principle from the two previous methods but is classified with them as it is partly a resonance method and does not involve any movement of the measuring instrument on the line.

A short-circuited transmission line of length l , less than $\frac{\lambda}{4}$, is used for the measurements. An electro-motive force is induced in the line through the shorting plate and the other end is closed by a variable condenser C across which a valve-voltmeter is connected (figure 1.5).

The shunt reactance X of the unknown impedance is first found by connecting the latter across C and tuning C for resonance as indicated by a maximum reading of the voltmeter. Let this value of C be C_1 . The impedance is then removed and C is again tuned for resonance at a value C_2 , say. The shunt reactance X then follows from the two values of **the** reactance of the tuned condenser.

$$\omega C_1 - \frac{1}{X} = \omega C_2 \quad \text{where} \quad \omega = 2\pi \times \text{frequency}$$

$$X = \frac{1}{\omega(C_1 - C_2)} \quad (1.22)$$

In order to obtain the shunt resistance of the unknown impedance it is first necessary to find an expression for

the voltage V_y at any point on the line distance y from one end in terms of y and l and the voltage V_i across the other end (see figure 1.5).

Referring back to equation (1.15), where K_G and K_T are the voltage reflection coefficients of the terminating impedances, the voltage at any point in the line distance x from one end is given by

$$V_x = \frac{\mathcal{E}_G Z_0}{Z_0 + Z_G} \left\{ e^{-\Gamma x} + (K_T e^{-2\Gamma l}) e^{\Gamma x} \right\} \\ 1 - K_G K_T e^{-2\Gamma l}$$

where the symbols have the same meaning as before (see figure 1.1)

Substituting $K_T = \frac{Z_T - Z_0}{Z_T + Z_0}$ and $K_G = \frac{Z_G - Z_0}{Z_G + Z_0}$

$$V_x = \frac{\mathcal{E}_G Z_0}{(Z_0 + Z_G)} \left\{ \frac{e^{-\Gamma x} + \frac{Z_T - Z_0}{Z_T + Z_0} e^{-2\Gamma l + \Gamma x}}{1 - \frac{(Z_G - Z_0)(Z_T - Z_0)}{(Z_G + Z_0)(Z_T + Z_0)} e^{-2\Gamma l}} \right\} \\ = \frac{\mathcal{E}_G Z_0}{(Z_0 + Z_G)} \left\{ \frac{(Z_T + Z_0) e^{\Gamma(l-x)} + (Z_T - Z_0) e^{-\Gamma(l-x)}}{(Z_G + Z_0)(Z_T + Z_0) e^{\Gamma l} - (Z_G - Z_0)(Z_T - Z_0) e^{-\Gamma l}} \right\} (Z_0 + Z_G) \\ = \mathcal{E}_G \cdot Z_0 \cdot \frac{Z_0 \sinh \Gamma(l-x) + Z_T \cosh \Gamma(l-x)}{Z_0 \{ Z_0 \sinh \Gamma l + Z_T \cosh \Gamma l \} + Z_G \{ Z_0 \cosh \Gamma l + Z_T \sinh \Gamma l \}} \quad (1.23)$$

The input impedance to the line is given by equation (1.16)

$$Z_i = \frac{Z_0 (1 + K_T e^{-2\Gamma l})}{(1 - K_T e^{-2\Gamma l})}$$

Substituting for K_T in this equation

$$\begin{aligned} Z_i &= Z_o \cdot \frac{(1 + \frac{Z_T - Z_o}{Z_T + Z_o} \cdot e^{-2Pl})}{(1 - \frac{Z_T - Z_o}{Z_T + Z_o} \cdot e^{-2Pl})} \\ &= Z_o \cdot \frac{\{(Z_T + Z_o)e^{Pl} + (Z_T - Z_o)e^{-Pl}\}}{\{(Z_T + Z_o)e^{Pl} - (Z_T - Z_o)e^{-Pl}\}} \\ &= Z_o \cdot \frac{\{Z_o \sinh Pl + Z_T \cosh Pl\}}{Z_o \cosh Pl + Z_T \sinh Pl} \end{aligned} \quad (1.24)$$

Substituting equation (1.24) into the denominator of equation (1.23) the latter becomes

$$Z_o \{Z_o \sinh Pl + Z_T \cosh Pl\} + Z_G \cdot \frac{Z_o}{Z_i} \{Z_o \sinh Pl + Z_T \cosh Pl\}$$

so that equation (1.23) may be written

$$V_x = E_G \cdot \frac{Z_i}{Z_i + Z_G} \cdot \frac{Z_o \sinh P(l-x) + Z_T \cosh P(l-x)}{Z_o \sinh Pl + Z_T \cosh Pl}$$

If the distances are now measured from the shorted end and the voltage across the other end is V_i (see figure 1.5)

then $l-x = y$ and $V_i = \frac{E_G \cdot Z_i}{Z_i + Z_G}$

$$\text{Thus } V_y = V_i \left\{ \frac{Z_o \sinh Py + Z_T \cosh Py}{Z_o \sinh Pl + Z_T \cosh Pl} \right\} \quad (1.25)$$

Where $V_y = V_x$.

In this case since the end is shorted $Z_T = 0$ and equation (1.25) reduces to

$$V_y = V_i \cdot \frac{\sinh Py}{\sinh Pl}$$

Substituting $P = \alpha + j\beta$ and neglecting line losses (i.e. putting $\alpha = 0$)

$$V_y = V_i \cdot \frac{\sin \beta y}{\sin \beta l}$$

To find the required shunt resistance, without the unknown impedance connected across C a known non-inductive resistance R' is connected across the line. By sliding this resistance along the line a position is found when the reading of V_i is the same as the original reading with the impedance connected across C. If R' is sufficiently large to have no effect on the voltage distribution along the line the power loss in the resistance can be expressed as

$$\frac{V_i^2}{R'} \left\{ \frac{\sin \beta y}{\sin \beta l} \right\}^2 \quad \text{where } l \text{ is the distance of } R' \text{ from the shorted end of the line.}$$

The power loss in the unknown shunt resistance R at the end of the line is $\frac{V_i^2}{R}$

So that by making these equal

$$R = R' \left\{ \frac{\sin \frac{2\pi}{\lambda} \cdot l}{\sin \frac{2\pi}{\lambda} y} \right\}^2 \quad \text{where } \beta = \frac{2\pi}{\lambda}$$

If $l \ll \frac{\lambda}{4}$ this can be put in the form

$$R = R' \left(\frac{l}{y} \right)^2$$

Miller and Salzberg worked at frequencies of 30-250 Mc/s and used a single copper rod above a plate for the lines. They first investigated the change in effective resistance of different types of fixed resistors throughout this frequency range. Later the method was used to measure the dielectric constant and power factor of insulators. The capacity of a condenser was found first with air and then with solid dielectric between the plates. If these values are C_1 and C_2 ,

respectively, the ratio $\frac{c_2}{c_1}$ gives the dielectric constant. The effective resistance r of the latter was then found as described so that the power factor δ is given by $\delta = \frac{1}{\omega c_2 r}$

In the second group of line methods of measuring impedances the measuring instrument is actually moved along the lines and the standing-wave pattern investigated. The earlier methods employed one measuring instrument only and an example of this type is the Brückmann⁵ method of impedance measurement. In the course of outlining the theory of the Miller and Salzberg method of measuring admittances an equation expressing the voltage V_y at any point on a line distance y from one end in terms of the voltage V_i at the other end was developed, viz

$$V_y = V_i \cdot \frac{Z_0 \sinh Py + Z_T \cosh Py}{Z_0 \sinh Pl + Z_T \cosh Pl} \quad (1.25)$$

At the end of the line $y = 0$ and the voltage at the termination V_T is given by

$$V_T = V_i \cdot \frac{Z_T}{Z_0 \sinh Pl + Z_T \cosh Pl} \quad (1.26)$$

Substitution from this equation in equation (1.25) gives

$$\begin{aligned} V_y &= V_T \left\{ \frac{Z_0}{Z_T} \sinh Py + \cosh Py \right\} \\ &= V_T \left\{ j \cdot \frac{Z_0}{Z_T} \sin \beta y + \cos \beta y \right\} \end{aligned}$$

(putting $P = \alpha + j\beta$ and neglecting line losses)

Hence when $\sin \beta y = 0$ (i.e. $y = \frac{n\lambda}{2}$), $\left| \frac{V_y}{V_T} \right| = 1$ (1.27)

and when $\cos \beta y = 0$ (i.e. $y = \frac{(2n+1)\lambda}{4}$), $\left| \frac{V_y}{V_T} \right| = \left| \frac{Z_o}{Z_T} \right|$

$$\therefore \left| \frac{V_{\frac{\lambda}{2}}}{V_{\frac{\lambda}{4}}} \right| = \left| \frac{Z_T}{Z_o} \right| \quad (1.28)$$

From this same equation

$$\frac{V_y}{V_T} = \left\{ \cos \beta y + j \frac{Z_o}{Z_T} \sin \beta y \right\}$$

Thus $\left| \frac{V_y}{V_T} \right|^2 = \left[\cos \beta y + \frac{j Z_o}{(R_T + j X_T)} \sin \beta y \right] \left[\cos \beta y - \frac{j Z_o}{(R_T - j X_T)} \sin \beta y \right]$

(substituting $Z_T = R_T + j X_T$ and treating Z_o as purely real)

$$\begin{aligned} \left| \frac{V_y}{V_T} \right|^2 &= \cos^2 \beta y + \frac{j Z_o \sin 2\beta y}{2(R_T + j X_T)} - \frac{j Z_o \sin 2\beta y}{2(R_T - j X_T)} + \frac{Z_o^2 \sin^2 \beta y}{|Z_T|^2} \\ &= \frac{\cos 2\beta y + 1}{2} + \frac{Z_o X_T \sin 2\beta y}{|Z_T|^2} + \frac{Z_o^2}{|Z_T|^2} \left[\frac{1 - \cos 2\beta y}{2} \right] \\ &= \frac{1}{2} \left\{ 1 + \frac{Z_o^2}{|Z_T|^2} + \cos 2\beta y \left(1 - \frac{Z_o^2}{|Z_T|^2} \right) + \frac{2 X_T Z_o \sin 2\beta y}{|Z_T|^2} \right\} \\ &= \frac{|Z_T|^2 + Z_o^2}{2|Z_T|^2} \left\{ 1 + \cos 2\beta y \cdot \frac{|Z_T|^2 - Z_o^2}{|Z_T|^2 + Z_o^2} + \frac{2 X_T Z_o \sin 2\beta y}{|Z_T|^2 + Z_o^2} \right\} \end{aligned}$$

Now introduce γ where $\tan \gamma = \frac{|Z_T|^2 - Z_o^2}{2 X_T Z_o}$

$$\begin{aligned} \text{i.e. } \sin \gamma &= \frac{|Z_T|^2 - Z_o^2}{\sqrt{|Z_T|^4 + Z_o^4 - 2 Z_o^2 (R_T^2 + X_T^2) + 4 X_T^2 R_T^2}} \\ &= \frac{|Z_T|^2 - Z_o^2}{\sqrt{|Z_T|^4 + Z_o^4 + 2 Z_o^2 (X_T^2 - R_T^2)}} \end{aligned}$$

$$\text{and } \cos \gamma = \frac{2 X_T Z_o}{\sqrt{|Z_T|^4 + Z_o^4 + 2 Z_o^2 (X_T^2 - R_T^2)}}$$

$$\begin{aligned} \text{Thus } \left| \frac{V_y}{V_T} \right|^2 &= \frac{|Z_T|^2 + Z_o^2}{2|Z_T|^2} \left\{ 1 + \frac{\sqrt{|Z_T|^4 + Z_o^4 + 2Z_o^2(X_T^2 - R_T^2)}}{(|Z_T|^2 + Z_o^2)} (\cos 2\beta y \sin \delta + \sin 2\beta y \cos \delta) \right\} \\ &= \frac{|Z_T|^2 + Z_o^2}{2|Z_T|^2} \left\{ 1 + \sqrt{\frac{(|Z_T|^2 + Z_o^2)^2 - 2Z_o^2(R_T^2 + X_T^2) + 2Z_o^2(X_T^2 - R_T^2)}{(|Z_T|^2 + Z_o^2)^2}} \cdot \sin(2\beta y + \delta) \right\} \\ &= \frac{|Z_T|^2 + Z_o^2}{2|Z_T|^2} \left\{ 1 + \sqrt{1 - \left(\frac{2Z_o R_T}{|Z_T|^2 + Z_o^2} \right)^2} \cdot \sin(2\beta y + \delta) \right\} \end{aligned}$$

Thus the maximum values of $\left| \frac{V_y}{V_T} \right|^2$ occur when

$$\begin{aligned} 2\beta y + \delta &= (2n + \frac{1}{4})\pi \\ \text{i.e. } y &= \frac{(2n + \frac{1}{4})\lambda}{4} + \frac{\delta \cdot \lambda}{4\pi} \end{aligned}$$

and are given by $\frac{|Z_T|^2 + Z_o^2}{2|Z_T|^2} \left\{ 1 + \sqrt{1 - \left(\frac{2Z_o R_T}{|Z_T|^2 + Z_o^2} \right)^2} \right\}$

and the minimum values occur when

$$y = \frac{(2n + \frac{3}{4})\lambda}{4} + \frac{\delta \lambda}{4\pi}$$

and are given by $\frac{|Z_T|^2 + Z_o^2}{2|Z_T|^2} \left\{ 1 - \sqrt{1 - \left(\frac{2Z_o R_T}{|Z_T|^2 + Z_o^2} \right)^2} \right\}$

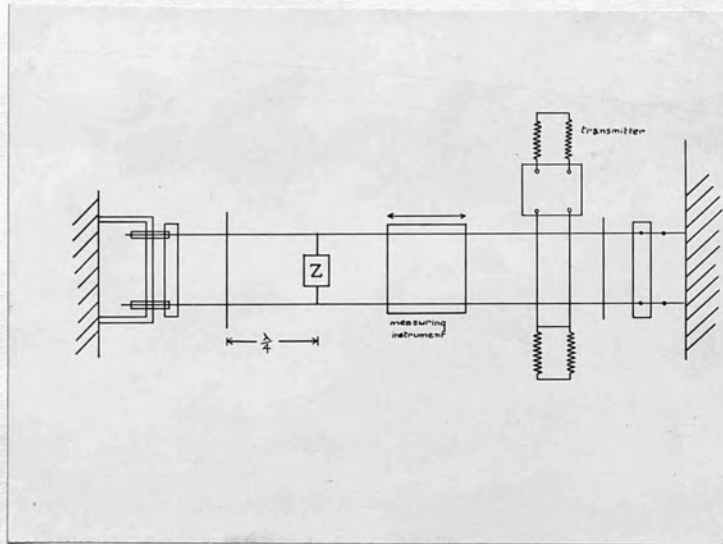
$$\begin{aligned} \text{Hence } \left\{ \left| \frac{V_{\max}}{V_T} \right| + \left| \frac{V_{\min}}{V_T} \right| \right\}^2 &= \left| \frac{V_{\max}}{V_T} \right|^2 + \left| \frac{V_{\min}}{V_T} \right|^2 + 2 \left| \frac{V_{\max}}{V_T} \right| \left| \frac{V_{\min}}{V_T} \right| \\ &= \frac{|Z_T|^2 + Z_o^2}{|Z_T|^2} + \frac{|Z_T|^2 + Z_o^2}{|Z_T|^2} \sqrt{1 - \left\{ 1 - \left(\frac{2Z_o R_T}{|Z_T|^2 + Z_o^2} \right)^2 \right\}} \\ &= 1 + \frac{Z_o^2}{|Z_T|^2} + \frac{2R_T Z_o}{|Z_T|^2} \\ &= 1 + \left| \frac{Z_o}{Z_T} \right|^2 + 2 \left| \frac{Z_o}{Z_T} \right| \cos \phi_T \end{aligned}$$

Where $\phi_T = \frac{R_T}{|Z_T|}$ and is the phase angle of the unknown

impedance, but $\frac{V_{\lambda/2}}{V_T} = 1$ and $\frac{V_{\lambda/4}}{V_{\lambda/2}} = \left| \frac{Z_T}{Z_o} \right|$ [equations (1.27) and (1.28)]

$$\text{i.e. } \frac{V_{\lambda/4}}{V_{\lambda/2}} = \left| \frac{Z_o}{Z_T} \right|$$

Figure (1.6)



by making these substitutions

$$\left\{ \left| \frac{V_{\max}}{V_T} \right| + \left| \frac{V_{\min}}{V_T} \right| \right\}^2 = \left| \frac{V_{\lambda/2}}{V_T} \right|^2 + \left| \frac{V_{\lambda/4}}{V_T} \right|^2 + 2 \left| \frac{V_{\lambda/2}}{V_T} \right| \left| \frac{V_{\lambda/4}}{V_T} \right| \cos \phi_T$$

$$\cos \phi_T = \frac{\left\{ |V_{\max}| + |V_{\min}| \right\}^2 - |V_{\lambda/2}|^2 - |V_{\lambda/4}|^2}{2 |V_{\lambda/2}| |V_{\lambda/4}|} \quad (1.29)$$

Similarly by calculating $\left\{ \left| \frac{V_{\max}}{V_T} \right| - \left| \frac{V_{\min}}{V_T} \right| \right\}^2$ in terms of

$$V_{\lambda/2}, V_{\lambda/4} \text{ and } \cos \phi_T$$

$$\cos \phi_T = \frac{|V_{\lambda/2}|^2 + |V_{\lambda/4}|^2 - \left\{ |V_{\max}| - |V_{\min}| \right\}^2}{2 |V_{\lambda/2}| |V_{\lambda/4}|} \quad (1.30)$$

Adding (1.29) and (1.30)

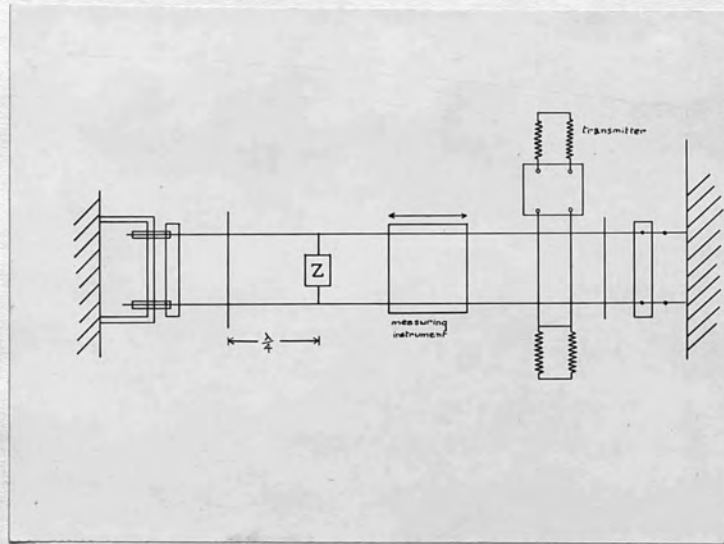
$$\cos \phi_T = \frac{|V_{\max}| |V_{\min}|}{|V_{\lambda/2}| |V_{\lambda/4}|} \quad (1.31)$$

Thus using equations (1.28) and (1.31) the modulus and phase angle of the unknown impedance can be found when the maximum and minimum voltages along the line and the voltages at distances of half a wavelength and a quarter of a wavelength from the terminating impedance are known.

Brückmann and Hempel used twin open lines for their experimental work on this method as shown in figure (1.6). The unknown impedance was connected at a voltage antinode.

The two disadvantages of this method as compared with resonance methods are firstly when the measuring instrument is moved along the line to investigate the wave pattern the input impedance of the line is altered and the power input into the measuring circuit is not constant and secondly the method is only suitable for the measurement of impedances of the same order of value as the characteristic impedance of the line

Figure (1.6)



by making these substitutions

$$\left\{ \left| \frac{V_{\max}}{V_T} \right| + \left| \frac{V_{\min}}{V_T} \right| \right\}^2 = \left| \frac{V_{\lambda/2}}{V_T} \right|^2 + \left| \frac{V_{\lambda/4}}{V_T} \right|^2 + 2 \left| \frac{V_{\lambda/2}}{V_T} \right| \left| \frac{V_{\lambda/4}}{V_T} \right| \cos \phi_T$$

$$\cos \phi_T = \frac{\left\{ |V_{\max}| + |V_{\min}| \right\}^2 - |V_{\lambda/2}|^2 - |V_{\lambda/4}|^2}{2 |V_{\lambda/2}| |V_{\lambda/4}|} \quad (1.29)$$

Similarly by calculating $\left\{ \left| \frac{V_{\max}}{V_T} \right| - \left| \frac{V_{\min}}{V_T} \right| \right\}^2$ in terms of

$$V_{\lambda/2}, V_{\lambda/4} \text{ and } \cos \phi_T$$

$$\cos \phi_T = \frac{|V_{\lambda/2}|^2 + |V_{\lambda/4}|^2 - \left\{ |V_{\max}| - |V_{\min}| \right\}^2}{2 |V_{\lambda/2}| |V_{\lambda/4}|} \quad (1.30)$$

Adding (1.29) and (1.30)

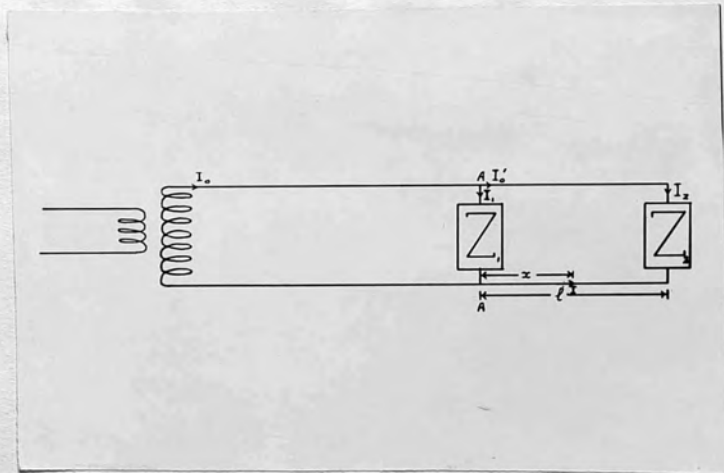
$$\cos \phi_T = \frac{|V_{\max}| |V_{\min}|}{|V_{\lambda/2}| |V_{\lambda/4}|} \quad (1.31)$$

Thus using equations (1.28) and (1.31) the modulus and phase angle of the unknown impedance can be found when the maximum and minimum voltages along the line and the voltages at distances of half a wavelength and a quarter of a wavelength from the terminating impedance are known.

Brückmann and Hempel used twin open lines for their experimental work on this method as shown in figure (1.6). The unknown impedance was connected at a voltage antinode.

The two disadvantages of this method as compared with resonance methods are firstly when the measuring instrument is moved along the line to investigate the wave pattern the input impedance of the line is altered and the power input into the measuring circuit is not constant and secondly the method is only suitable for the measurement of impedances of the same order of value as the characteristic impedance of the line

Figure (1.7)



since it is only in this case that the standing wave pattern is suitable for measurements. On the other hand the resonance methods, as mentioned before, have not been found suitable for the measurement of high values of impedance because of the damping effect on the resonance curve. This makes resonance methods unsuitable for measuring the conductivity and dielectric constant of liquids.

There is a further method for the measurement of impedance using Lecher Wires which is suitable for high values of impedance namely that of Flint and Williams⁶. This method possesses the further advantage that the measurements taken are independent of random fluctuations of the input power as well as variations due to changes of the input impedance of the lines.

A diagrammatic sketch of the apparatus is shown in figure (1.7). The two impedances Z_1 and Z_2 refer to those of two vacuum thermo-junctions whose couples are connected to sensitive micro-ammeters. The latter record a quantity proportional to the square of the currents I_1 and I_2 flowing in Z_1 and Z_2 . It is the ratio I_1^2/I_2^2 which is required and this is independent of input power and does not depend on the meter constants. In the calculation the symbols have the same meanings as before and any new notation is explained by the diagram. Current reflection coefficients are used and K_1 and K_2 are the current reflection coefficients

of the impedances Z_1 and Z_2 .

$$\text{Hence } K_1 = \frac{Z_0 - Z_1}{Z_0 + Z_1} \quad \text{and} \quad K_2 = \frac{Z_0 - Z_2}{Z_0 + Z_2} \quad (1-32)$$

The equations for current and voltage \bar{I}_x and V_x at any point on the line are given by equation (1.1)

$$V_x = \frac{\mathcal{E}_G \cdot \frac{Z_0}{Z_0 + Z_2} \{e^{-Px} (K_2 e^{-2Pl}) e^{Px}\}}{1 - K_1 K_2 e^{-2Pl}}$$

$$\bar{I}_x = \frac{1}{Z_0} \cdot \frac{\mathcal{E}_G \cdot \frac{Z_0}{Z_0 + Z_2} \{e^{-Px} + (K_2 e^{-2Pl}) e^{Px}\}}{1 - K_1 K_2 e^{-2Pl}}$$

The voltage V_A across the line at AA can be found by putting $x=0$ in this expression. The further substitution of $V_A = \bar{I}_1 Z_1$

gives

$$\bar{I}_1 = \frac{\mathcal{E}_G \cdot \frac{Z_0}{Z_0 + Z_2} \{1 - K_2 e^{-2Pl}\}}{1 - K_1 K_2 e^{-2Pl}} \cdot \frac{1}{Z_1}$$

and substitution of $x=1$ in the equation for \bar{I}_x gives

$$\bar{I}_2 = \frac{1}{Z_0} \cdot \frac{\mathcal{E}_G \cdot \frac{Z_0}{Z_0 + Z_2} \{e^{-Pl} + K_2 e^{-Pl}\}}{1 - K_1 K_2 e^{-2Pl}}$$

$$\therefore \frac{\bar{I}_1}{\bar{I}_2} = \frac{Z_0}{Z_1} \cdot \frac{e^{Pl} - K_2 e^{-Pl}}{(1 + K_2)}$$

putting $K_2 = e^{-2P}$

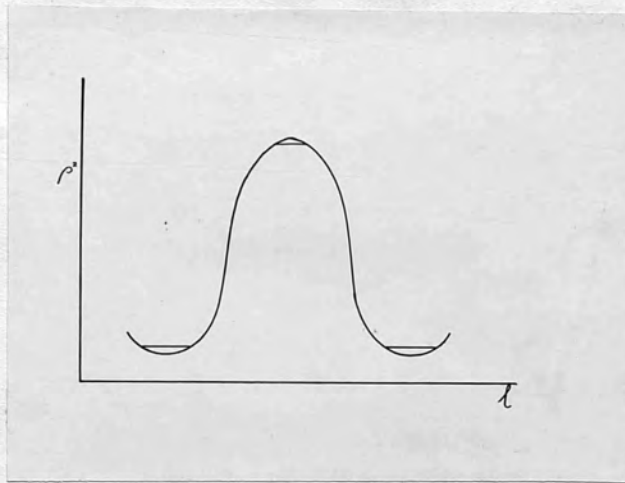
$$\frac{\bar{I}_1}{\bar{I}_2} = \frac{Z_0}{Z_1} \cdot \frac{e^{-P}}{(1 + K_2)} \cdot (e^{(Pl+P)} - e^{-(Pl+P)})$$

$$= \frac{2Z_0}{Z_1} \cdot \frac{e^{-P}}{1 + K_2} \cdot \sinh(Pl+P)$$

Now write

$$\rho^2 = \left| \frac{\bar{I}_1}{\bar{I}_2} \right|^2$$

Figure (1.8)



It is this quantity that is actually observed

$$\rho^2 = A |\sinh(P\ell + \gamma)|^2$$

where A is independent of the value of l.

Further substitution of $(a + jb)$ for the complex quantity τ

and of $j\beta$ for P (i.e. attenuation is neglected) gives

$$\begin{aligned} \rho^2 &= A |\{\sinh a \cos(b + \beta l) - j \cosh a \sin(b + \beta l)\}|^2 \\ &= A \{\sinh^2 a \cos^2(b + \beta l) + \cosh^2 a \sin^2(b + \beta l)\} \\ &= A \{\sinh^2 a + \sin^2(b + \beta l)\} \end{aligned}$$

The maxima of ρ are given by

$$\rho_{\max}^2 = A \cosh^2 a$$

and they occur when

$$b + \beta l = \frac{(2n+1)\pi}{2} \quad \text{where } n \text{ is any integer}$$

$$\begin{aligned} \text{Hence } 1 - \left(\frac{\rho}{\rho_{\max}}\right)^2 &= 1 - \frac{\sinh^2 a + \sin^2(b + \beta l)}{\cosh^2 a} \\ &= \frac{\cos^2(b + \beta l)}{\cosh^2 a} \end{aligned} \quad (1.33)$$

This equation shows that a graph of ρ^2 against l is symmetrical about the turning points.

$$\text{Similarly } \rho_{\min}^2 = A \sinh^2 a$$

(since ρ_{\min} occurs where $b + \beta l = n\pi$)

$$\text{Thus } \rho_{\min} = \rho_{\max} \tanh a$$

The readings of ρ^2 are plotted against those of l and a curve of the shape shown in figure (1.8) is obtained. The distance between successive maxima and minima gives the value of $\frac{\lambda}{4}$. The positions are found accurately by plotting mean abscissae near the turning points. The value of b is obtained

from the fact that the first maximum occurs when $b + \beta z = \frac{\pi}{2}$ and this can be checked by the position of the first minimum. The value of a is found by plotting a graph of $\cos^2(b + \beta z)$ against z^2 . From equation (1.33) this can be seen to be a straight line with intercept $\cosh^2 a$ on the $\cos^2(b + \beta z)$ axis.

Knowing a and b , Z_2 can be calculated from the current reflection coefficient since

$$K_2 = \frac{Z_0 - Z_2}{Z_0 + Z_2} = e^{-2\gamma} = e^{-2(a+jb)}$$

$$\therefore \frac{Z_2}{Z_0} = \frac{e^{-2(a+jb)} - 1}{1 - e^{-2(a+jb)}}$$

i.e. $Z_2 = Z_0 \tanh(a+jb)$

If Z_0 is purely resistive

$$Z_2 = \frac{Z_0(\tanh a + j \tan b)}{1 + j \tanh a \tan b} = \frac{Z_0(\tanh a + j \tan b)(1 - j \tanh a \tan b)}{1 + \tanh^2 a \tan^2 b}$$

The real or resistive component of Z_2 is therefore

$$Z_0 \frac{\tanh a + \tanh^2 a \tan^2 b}{1 + \tanh^2 a \tan^2 b} = Z_0 \frac{\tanh^2 a \sec^2 b}{1 + \tanh^2 a \tan^2 b}$$

and the unreal or reactive component is

$$Z_0 \frac{\tan b(1 - \tanh^2 a)}{1 + \tanh^2 a \tan^2 b} = Z_0 \frac{\tan b \operatorname{sech}^2 a}{1 + \tanh^2 a \tan^2 b}$$

In the experimental work described in the original paper on this method the impedances of several current meters were measured at a frequency of about 150 Mc/s. If any other unknown impedance is to be found it must be put in parallel with the current meter at the end of the line and the impedance of the latter determined first by a separate experiment.

The sensitivity of this method has been investigated by

Rogers⁷. His analysis shows that a , which is difficult to measure when small, is a maximum when $b = 45^\circ$ and this occurs when the modulus of the unknown impedance equals that of the characteristic impedance of the line. Since it is difficult to construct a line with a characteristic impedance greater than about 500 ohms this makes the method insensitive for impedances with large phase angle. In order to reduce the phase angle however the impedance may be shunted by a variable length of short-circuited line but this makes the experimental technique lengthy and intricate.

The Flint and Williams method was used by Rogers and Williams⁸ to investigate the impedances of thermo-junctions of nominal resistances from 600 to 1600 ohms at 150 Mc/s.

ρ^2/s curves were plotted firstly with the thermo-junctions mounted in pin-bases in valve holders and secondly connected directly to the line (a system of Lecher wires). The curves shifted to the right when the thermo-junctions were dismantled and the capacitative effect due to the holder was thus calculated to be of the order of 1 pf. Also by investigating thermo-junctions of different resistance it was shown that the residuals of reactance were inductive for low values of resistance and capacitative for high values of resistance. Thus as the resistive component increases due to the skin-effect it is nullified by the net increase of self-capacity and the resultant impedance is less at higher

frequencies.

A variation of the method in which the unknown impedance is determined without a knowledge of that of the current meter is due to Williams⁹. In this case the impedance is connected across the end of the wires and two current meters are kept a fixed distance apart and moved along the line together. As in the previous method it is the ratio of the currents flowing that is required and consequently there are no errors due to variations of the input power. This method is described in detail in Section III and will not be considered further here.

In conclusion it appears that the principal sources of error inherent in the various methods may be summarised as follows. If a single meter is used to investigate the standing-wave-pattern along a line terminated in an unknown impedance the input impedance of the line alters with the movement of the meter and thus the power input into the lines varies apart from any random power fluctuations. Also the method is only suitable when the unknown impedance~~s~~ approximates to the characteristic impedance of the line.

Resonance methods depend upon a perfectly stable power input. They are not suitable for measuring impedances which are near the value of the characteristic impedance of the line or for very high impedances.

The methods employing two meters are independant of a

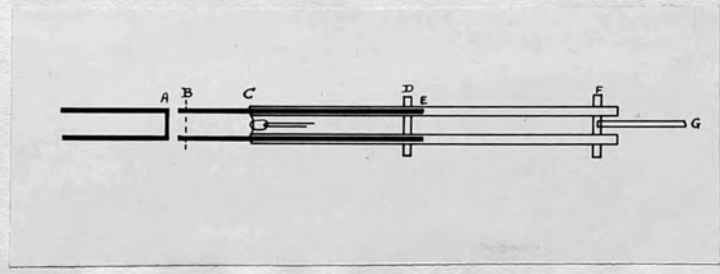
steady power input and can be used for higher values of impedance although the most accurate results are obtained when the impedance is near that of the characteristic impedance of the lines. The experimental technique is longer and more tedious than in the other methods.

The methods mentioned in the last two paragraphs both necessitate shorting the end of the line. Perfect reflection may be difficult to attain and this will be a further source of errors.

SECTION II

THE CURRENT RESONANCE METHOD FOR THE
MEASUREMENT OF IMPEDANCES

Figure (2.1)



a) CHIPMAN'S METHOD

The general theory of the Chipman method of impedance measurement by the use of current resonance was given among the methods in Section I. The original apparatus and experimental technique will be described in this section. In his introduction to the paper Chipman stresses the importance of the method for the measurement of impedances which are not necessarily of the same order of magnitude as the characteristic impedance of the line. In previous methods involving measurements of the standing wave pattern on a line terminated by the unknown impedance it was only under these conditions that the readings of minimum voltage or current were not too small for accurate observation. Chipman states that the possible accuracy of the current resonance method varies approximately inversely as the frequency and is about 1% at 300 Mc/s.

The experimental arrangement is shown diagrammatically in figure (2.1). The thermocouple for detecting current was fixed to the outer tubes of the line and was therefore kept at a fixed distance from D and F. CD and DF were about a quarter of a wavelength and half a wavelength respectively. The line length l of figure (1.1) corresponds to BC in figure (2.1) and the shorting plates D and F ensured that the whole of the wave reaching C was reflected back and none of it travelled further down the line. The line was supported

Figure (2.2)

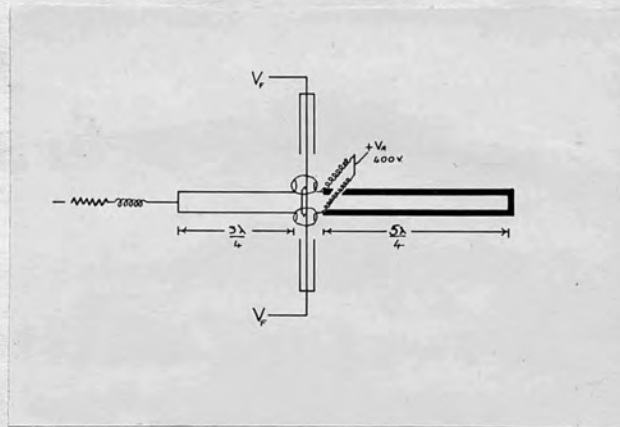
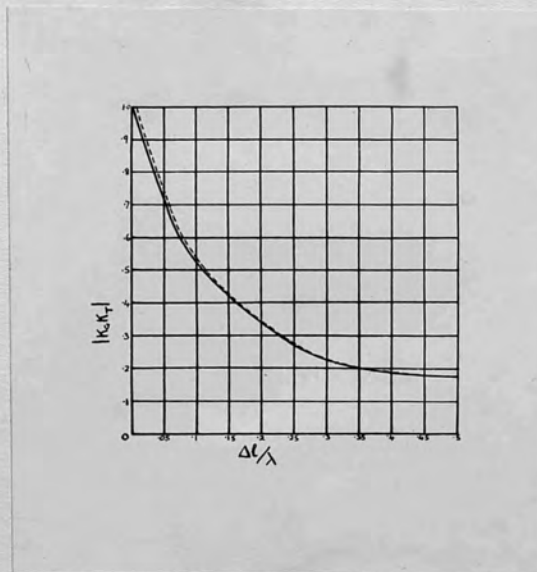


Figure (2.3)



by insulating pillars at a voltage antinode near B and also between D and E. The line length was altered by turning the screw ~~the~~ ^{of} the comparator to which the point G was connected and variations in line length were read on the comparator vernier. The oscillator A supplied electro-motive force at a frequency of 377 Mc/s. It was of the push-pull type and the circuit is shown in figure (2.2).

Referring back to the theory of the method in Section I, equations (1.8) and (1.9) reduce to equation (1.10).

$$\text{viz } \sinh^2(\alpha l_0 + p) + \sin^2 \frac{2\pi l}{\lambda} \cdot \delta l = \left\{ \sinh^2(\alpha l_0 + p) \right\} g^2$$

provided α the attenuation constant of the lines is sufficiently small. This equation was used to calculate the real part of the product of the reflection coefficients of the two terminating impedances, since

$$K_G K_T = e^{-2(p+jq)} \quad \text{i.e. } p = \log_e \frac{1}{|K_G K_T|^{\frac{1}{2}}} \quad (1.4)$$

A curve was plotted with $\frac{\Delta l}{\lambda}$ as abscissae and $|K_G K_T|$ as ordinates (figure (2.3)). $\Delta l = 2 \delta l =$ width of resonance curve where the current I is $\frac{1}{\sqrt{2}} \cdot I_{\max}$ (i.e. $I^2 = \frac{1}{2} \cdot I_{\max}^2$).

$|K_G K_T|$ could thus be read off the curve when Δl had been determined experimentally. Two curves were plotted as shown in figure (2.3), the full one of equation (1.10) (i.e. on the assumption that $\alpha = 0$) and the broken one of the sum of equations (1.8) and (1.9) taking $\alpha = 5 \times 10^{-4}$ nepers/cm. The validity of the assumption that $\alpha = 0$ was investigated and it was concluded that the final ratio $\frac{|K_G K_T|}{|K_T|}$ that was required was

$$\frac{|K_G K_T|}{|K_T|}$$

independent of which of the two curves was used with attenuation constants that are likely to be found in practice.

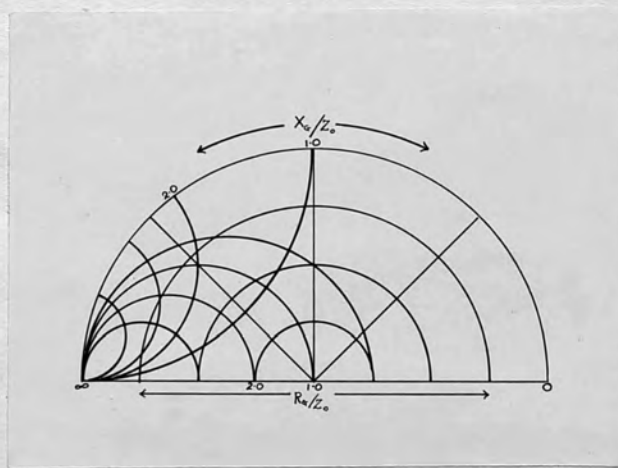
It was also concluded that for this value of α used at a frequency of 377 Mc/s the error introduced into the phase angle of the reflection coefficient by assuming a symmetrical resonance curve was less than experimental errors to be expected in measurements made on the resonance curve. The effect of radiation resistance on the attenuation constant was investigated and it was found that at the frequency used the distributed radiation resistance of the line was small enough for the attenuation constant still to be neglected and that the radiation resistance of the termination could be calculated from the formula $R_{rad} = \frac{80\pi^2 l^2}{\lambda^2}$ (where l in this case refers to the centre spacing of the line conductors).

When α is negligible $|K_G K_T|$ can be found another way by measurements made on maximum and minimum values of the current. This method was only used when the terminating impedance was resistive and of approximately the same value as the characteristic impedance of the line. In this case the current resonance method is least accurate and the method which follows is possible because the two currents are of the same order of magnitude. From equations (1.2), (1.4) and (1.5)

$$\text{viz } I_\ell = I_0 f(\ell) \quad ; \quad K_G K_T = e^{-2(p+j\gamma)\ell}$$

$$\text{and } f(\ell) = \frac{1}{2 \{ |K_G K_T| \sinh^2(\alpha\ell + p) + |K_G K_T| \sin^2(\beta\ell + \gamma\ell) \}^{\frac{1}{2}}}$$

Figure (2.4)



$$\bar{I}_\ell = \bar{I}_o \cdot \frac{1}{2 \left\{ |K_G K_T| \left(\frac{|K_G K_T|^{-\frac{1}{2}} - |K_G K_T|^{\frac{1}{2}}}{2} \right)^2 + |K_G K_T| \sin^2(\beta l + q) \right\}^{\frac{1}{2}}}$$

(putting $\alpha = 0$ and substituting for p).

The maximum value of \bar{I}_ℓ occurs when $(\beta l + q) = n\pi$ and the minimum value where $(\beta l + q) = \frac{(2n-1)\pi}{2}$

Hence $\bar{I}_{\max} = \frac{\bar{I}_o}{1 - |K_G K_T|}$ and $\bar{I}_{\min} = \frac{\bar{I}_o}{1 + |K_G K_T|}$

$$\therefore \frac{\bar{I}_{\max}}{\bar{I}_{\min}} = \frac{1 + |K_G K_T|}{1 - |K_G K_T|}$$

$$|K_G K_T| = \frac{\bar{I}_{\max} - \bar{I}_{\min}}{\bar{I}_{\max} + \bar{I}_{\min}}$$

For the calculation of the unknown impedance $Z_G (= R_G + jX_G)$

from its reflection coefficient and the characteristic

impedance of the line, equation (1.14) was used

viz $R_G = Z_o \left\{ \frac{1 - A^2 - B^2}{1 + A^2 + B^2 + 2A} \right\}$ where $\begin{cases} A = |K_G| \cos \phi_G \\ B = |K_G| \sin \phi_G \end{cases}$

$X_G = Z_o \left\{ \frac{2B}{1 + A^2 + B^2 + 2A} \right\}$

Curves of R_G/Z_o and X_G/Z_o were plotted on co-ordinates of K_G and ϕ_G (concentric circles and radial lines respectively). A sketch of the diagram is shown in figure (2.4)

Its use is similar to that of the more usual type of circle diagram¹⁰. The diagram is symmetrical about the base line

and, because of this, if any two impedances are connected by the relationship $Z_G \cdot Z_G' = Z_o^2$ the two points on the diagram

corresponding to these impedances are mirror images of each other in the base line. Hence the resonance curves of the two impedances are identical in shape and the possible accuracy of measurement of the magnitude and phase angle of each is the same. This property enabled measurements of known impedances less than the characteristic impedance of the line to be used to check the accuracy of the method over the whole impedance range.

Chipman states in his conclusion that an accuracy of more than 1% is obtainable in the determination of impedances except in the case when the impedance approximates to a resistance of the same value as the characteristic impedance of the line. In this case the product of the two reflection coefficients can be found from maximum and minimum current measurements but in these circumstances it is preferable, if possible, to alter the characteristic impedance of the line by varying the spacing and to use the resonance method.

b) ESSEN'S EXPERIMENTAL STUDY OF CHIPMAN'S METHOD.

The Chipman method of impedance measurement has been used by Essen¹¹ at frequencies above 400 Mc/s, the main application being the measurement of the propagation constants of radio-frequency cables. The accuracies achieved were $\pm 2\%$ for reactance and $\pm 5\%$ for resistance except when the unknown impedance was largely resistive and near the characteristic impedance of the line.

In most of Essen's calculations the simplified equation (1.10) of Chipman's calculation

$$\text{viz } \sinh^2(\alpha l_0 + p) + \sin^2 \beta \delta l = \{ \sinh^2(\alpha l_0 + p) \} g^2$$

was further simplified to

$$\sqrt{g^2 - 1} = \frac{\sin \beta \delta l}{\sinh p} \quad (2.1)$$

i.e. αl_0 was neglected in comparison with p .

$$\text{Also since } K_T K_G = e^{-2(p + j\gamma)} \quad (1.4)$$

$$|K_T K_G| = e^{-2p} \quad \text{i.e. } p = -\frac{1}{2} \log_e |K_T K_G|$$

If g^2 is taken as two for both resonance curves (i.e. with

Z_G and with a shorting plate connected across the input end of the line), substituting for p from equation (2.1)

$$|K_G| = \text{antilog } 2 \{ \sinh^{-1}(\sin \beta \delta l_{s.c.}) - \sinh^{-1}(\sin \beta \delta l) \} \quad (2.2)$$

where δl and $\delta l_{s.c.}$ are the resonant half-widths of the curves in the two cases.

This equation and equation (1.12) viz $\phi_G = \frac{4\pi}{\lambda} (l_{s.c.} - l_0)$ were found most generally useful for calculating $|K_G|$ and ϕ , instead of using the curves of $|K_G K_T|$ against $\frac{\Delta l}{\lambda}$ plotted by

Figure (2.5)

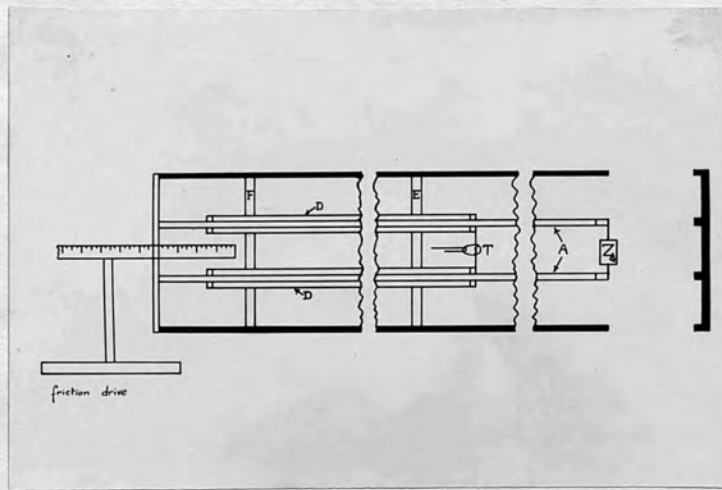
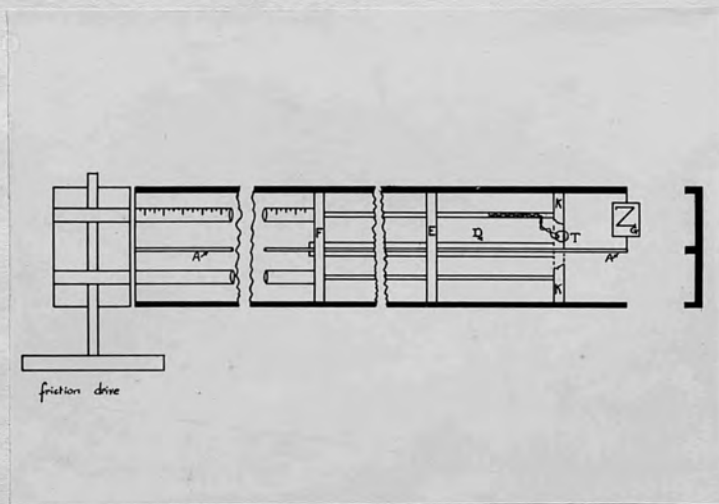


Figure (2.6)



Chipman (figure 2.3), when an accuracy of 2% was all that was required. The resistive and reactive components of the unknown impedance were calculated from its reflection coefficient and phase angle by using the circle diagram described in Chipman's work (figure 2.4).

Considering equation (1.14) for the reactance of the unknown impedance

$$\text{viz } X_G = \pm Z_0 \left\{ \frac{2B}{1 + A^2 + B^2 + 2A} \right\}$$

and substituting for A and B

$$X_G = \pm Z_0 \left\{ \frac{2|K_G| \sin \phi_G}{1 + |K_G|^2 + 2|K_G| \cos \phi_G} \right\}$$

when $|K_G| = 1$ this reduces to $X_G = Z_0 \tan \frac{\phi_G}{2}$

Substituting for ϕ_G from equation (1.12)

$$X_G = Z_0 \tan \frac{2\pi}{\lambda} (l_{s.c.} - l_0)$$

From this equation it can be seen that for the measurement of impedances varying in size from plus infinity to minus infinity a line of length $\frac{\lambda}{2}$ is required.

Essen used two types of closed line for his experimental work. Balanced impedances were measured on a screened twin line and unbalanced impedances on a coaxial line (figures (2.5) and (2.6))

In the screened twin line of figure (2.5) two brass conductors A were fixed to the brass end closing the brass outer screen. T was a thermo-junction (d.c. heater 3.3 ohms) connected between two lengths of tubing D, sliding on the

conductors A on narrow collars. Either the unknown impedance Z_G or the short-circuiting plate was connected at the end of the conductors. E and F were two heavy brass short-circuiting bridges sweated on to D and making sliding contact with the outer screen. These were found to be such efficient reflectors that their exact position along the line was not important and did not have to be adjusted for different frequencies. The variation in length of the line was 40 cm. so that the apparatus could be used for any frequency above 375 Mc/s.

Figure (2.6) is a sketch of the unbalanced line in which the lettering corresponds with that used for the balanced line. The contacts between the inner and outer conductors were made by a metal ring K, to which the thermo-junction unit T was attached, and by two short-circuiting discs E and F which were joined by three brass tubes.

The validity of certain assumptions in the theory of the method ~~was~~^{was} checked using this apparatus. First the attenuation constant of the line was measured to verify that it can be neglected in comparison with the experimental errors when taking measurements. Two resonance peaks a distance $\frac{\lambda}{2}$ apart were plotted and the resonant half-widths of the curves δl_1 and δl_2 measured. From equation (1.10)

$$\sqrt{g-1} = \frac{\sin \beta \cdot \delta l_1}{\sinh(\alpha l_0 + p)} = \frac{\sin \beta \delta l_2}{\sinh[\alpha(l_0 + \frac{\lambda}{2}) + p]}$$

where l_0 was the position of the first resonance peak.

Putting $g = 2$ and assuming p is small

$$\begin{aligned}\sin \beta \cdot Sl_1 &= \alpha l_0 + p \\ \sin \beta \cdot Sl_2 &= \alpha l_0 + \frac{\alpha \lambda}{2} + p \\ \therefore \alpha &= \frac{2(\sin \beta \cdot Sl_2 - \sin \beta \cdot Sl_1)}{\lambda}\end{aligned}$$

Essen's values for α were 1×10^{-4} nepers/cm for the balanced line and 1.5×10^{-4} nepers/cm for the unbalanced line.

In the theory of the method the reflection coefficient of the short-circuit which replaces the unknown impedance is always assumed to be unity. Essen checked this point experimentally in two ways. Firstly the inductance of a short-circuiting bar was measured by shorting 30 cm of line with two similar bars and measuring the resonant frequency. This was not quite 500 Mc/s (the latter corresponds to $\frac{\lambda}{2} = 30$ cm) and from the difference between $\frac{\lambda}{2}$ and 30 cm. the inductance was measured. This value was then compared with that obtained by using the bar as the unknown impedance in the Chipman method assuming that the short-circuit which replaced it was perfect. Secondly the inductances of several lengths of copper wire were calculated and then measured by the Chipman method with the same assumption. The results showed that the resonant length of line, when the end was short-circuited, was not in error by more than 0.15 cm in the case of the balanced line and 0.06 cm in that of the unbalanced line.

Measurements were made on the widths of the resonance

curves to find the radiation resistance of the short-circuiting plate. The mean of the half-widths of two resonance curves for open circuit was first found. This exceeded the half-width when the line was shorted by the plate by 0.085 cm. This was substituted in equations (1.10) and (1.14) to get the radiation resistance which was of the order of 0.2 ohms.

The average difference between the resonant lengths of short-circuited and open-circuited line differs from $\frac{\lambda}{4}$ by 0.35 cm. Neglecting the possible error due to the short-circuited line this corresponds to an open-circuit end effect of about 0.08 pf for the unbalanced line. Similar measurements for the balanced line gave an effect of 0.05 pf. This end-effect and also the impedance of any connecting wires are all included in the measurement of the unknown impedance.

The main use of the apparatus was for the measurement of the characteristic impedance and propagation constant of cables. The input impedance Z_i of a length of line l is given by equation (1.24)

$$\text{viz } Z_i = Z_0 \frac{\{Z_0 \sinh Pl + Z_T \cosh Pl\}}{Z_0 \cosh Pl + Z_T \sinh Pl}$$

When the line is shorted at one end $Z_T = 0$ and $Z_i = Z_{s.c.}$ say

$$\text{Thus } Z_{s.c.} = Z_0 \tanh Pl$$

Similarly when the line is on open circuit $Z_T \rightarrow \infty$

$$\text{and } Z_{o.c.} = Z_0 \coth Pl$$

$$\text{Thus } Z_0 = \sqrt{Z_{s.c.} \cdot Z_{o.c.}} \quad (2.3)$$

and $\tanh \Gamma l = \sqrt{Z_{s.c.}/Z_{o.c.}}$

Putting $\tanh \Gamma l = \tanh (\alpha + j\beta)l = A + jB$

α and β can be expressed in terms of A and B

viz
$$\tanh 2\alpha l = \frac{2A}{1+A^2+B^2} \quad (2.4)$$

$$\tan 2\beta l = \frac{2B}{1-A^2-B^2} \quad (2.5)$$

Thus using equations (2.3), (2.4) and (2.5), Z_0 , α and β could be calculated when $Z_{o.c.}$ and $Z_{s.c.}$ had been measured by the Chipman method.

Essen shows in an appendix to the paper that the measurement of resonant length is most accurate and the error due to the junction is a minimum when $Z_{s.c.}$ and $Z_{o.c.}$ are approximately equal and opposite in which case the length of the cable is $\frac{(2n+1)\lambda_c}{8}$ where λ_c is the wavelength in the cable. This condition may be satisfied by varying either frequency or length of line.

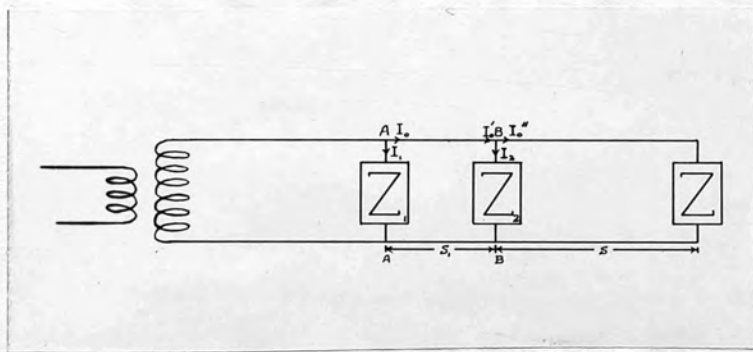
The value obtained for Z_0 when the signs of $Z_{s.c.}$ and $Z_{o.c.}$ were reversed (by variation of frequency) was not the same. This was because of the error due to the effective impedance at the short-circuited and open-circuited ends of the cable and was eliminated to a first order by taking a mean value. The attenuation varies with frequency so it was taken to apply to the mean frequency but it was necessary to determine the phase constant or wavelength and hence the velocity had to

be determined separately for each frequency. This was done by cutting successive lengths from the cable in such a way that in each case the reactance was zero. The length of cable removed each time was therefore $\frac{\lambda_c}{2}$ and the velocity could be calculated without any error due to end effect.

SECTION III

THE DOUBLE BRIDGE METHOD FOR THE MEASUREMENT
OF IMPEDANCES

Figure (3.1)



a) WILLIAMS' METHOD

Williams' method for the measurement of impedance by a system of Lecher wires was mentioned at the end of Section I. Two meters are moved along the line together and the ratio of the currents flowing in them noted. Similarly to the Flint and Williams' method the readings are independent of random fluctuations of input voltage and the method possesses the further advantage that a knowledge of the impedance of the current meter is not necessary.

A diagram of the apparatus is shown in figure (3.1).

Z_1 and Z_2 are the impedances of the current meters and Z is the unknown impedance. The meaning of the other symbols is clear from the diagram. The input impedance of the circuit beyond B and including Z but not Z_2 is given by equation (1.16) and is therefore

$$Z_0 \frac{(1 + Ke^{-2Ps})}{1 - Ke^{-2Ps}}$$

K is the reflection coefficient of the unknown impedance and putting $K = e^{-2\gamma}$, say, the input impedance beyond B becomes

$$Z_0 \tanh (Ps + \gamma)$$

Thus the total impedance beyond B including Z_2 is given by

$$\frac{Z_2 Z_0 \tanh (Ps + \gamma)}{Z_2 + Z_0 \tanh (Ps + \gamma)} = Z', \text{ say.} \quad (3.1)$$

Now considering the length AB of the line, from equation (1.26)

$$V_B = V_A \left\{ \frac{Z'}{Z_0 \sinh Ps_1 + Z' \cosh Ps_1} \right\} \quad (3.2)$$

where V_A is the voltage across the line at A

and V_B is the voltage across the line at B

$$\left. \begin{aligned} V_A &= \bar{I}_1 Z_1 \\ V_B &= \bar{I}_2 Z_2 \end{aligned} \right\} \begin{array}{l} \text{where } \bar{I}_1 \text{ and } \bar{I}_2 \text{ are the currents} \\ \text{flowing in } Z_1 \text{ and } Z_2. \end{array}$$

$$\therefore \frac{\bar{I}_1}{\bar{I}_2} = \frac{Z_2}{Z_1} \cdot \frac{V_A}{V_B}$$

Substituting for $\frac{V_A}{V_B}$ from equation (3.2)

$$\frac{\bar{I}_1}{\bar{I}_2} = \frac{1}{Z_1} \left\{ Z_2 \cosh Ps_1 + \frac{Z_2 Z_0}{Z'} \sinh Ps_1 \right\}$$

and for Z' from equation (3.1)

$$\frac{\bar{I}_1}{\bar{I}_2} = \frac{1}{Z_1} \left\{ Z_2 \cosh Ps_1 + Z_2 \sinh Ps_1 \coth(Ps_1 + \gamma) + Z_0 \sinh Ps_1 \right\}$$

Putting $\begin{cases} P = j\beta & (\text{i.e. neglecting attenuation}) \\ Z_2 = R_2 + jX_2 \\ \gamma = a + jb \end{cases}$

$$\frac{\bar{I}_1}{\bar{I}_2} = \frac{1}{Z_1} \left\{ (R_2 + jX_2) \cos \beta s_1 + jZ_0 \sinh Ps_1 + j(R_2 + jX_2) \sin \beta s_1 + \coth[a + j(bt + \beta s)] \right\}$$

This equation can be written in the form

$$\frac{\bar{I}_1}{\bar{I}_2} = \frac{1}{Z_1} \left\{ A + jB + (C + jD) \coth[a + j(bt + \beta s)] \right\}$$

where A, B, C and D depend only on Z_2 and s_1 , and are independent of Z and S .

$$\begin{aligned} A &= R_2 \cos \beta s_1 & B &= X_2 \cos \beta s_1 + Z_0 \sin \beta s_1 \\ C &= -X_2 \sin \beta s_1 & D &= R_2 \sin \beta s_1 \end{aligned}$$

Putting $\left| \frac{I_1}{I_2} \right|^2 = \rho^2$ and rationalizing

$$\rho^2 |Z_1|^2 = [(A+jB) + (C+jD)\coth\{a+j(b+\beta s)\}] [(A-jB) + (C-jD)\coth\{a-j(b+\beta s)\}]$$

$$= A^2 + B^2 + (AC+BD)\{\coth[a+j(b+\beta s)] + \coth[a-j(b+\beta s)]\} \\ + j(AD-BC)\{\coth[a+j(b+\beta s)] - \coth[a-j(b+\beta s)]\} \\ + (C^2+D^2)\coth[a+j(b+\beta s)] \cdot \coth[a-j(b+\beta s)]$$

$$= A^2 + B^2 + \frac{(AC+BD)\{2\operatorname{tanh}a + 2\operatorname{tanh}a \tan^2(b+\beta s)\} + (AD-BC)\{2\tan(b+\beta s) - 2\tan(b+\beta s)\operatorname{tanh}^2a\}}{\operatorname{tanh}^2a + \tan^2(b+\beta s)} + \\ \frac{(C^2+D^2)(1 + \operatorname{tanh}^2a \tan^2(b+\beta s))}{\operatorname{tanh}^2a + \tan^2(b+\beta s)}$$

$$= A^2 + B^2 + (C^2+D^2) + \frac{(C^2+D^2)\sec^2(b+\beta s)(1 + \operatorname{tanh}^2a) + (AC+BD)2\operatorname{tanh}a \sec^2(b+\beta s) + (AD-BC)2\tan(b+\beta s)\operatorname{sech}^2a}{\operatorname{tanh}^2a + \tan^2(b+\beta s)}$$

(multiplying by $\cosh^2 a \cdot \cos^2(b+\beta s)$)

$$= A^2 + B^2 - (C^2+D^2) + \frac{(C^2+D^2)\cosh 2a + (AC+BD)\sinh 2a + (AD-BC)\sin 2(b+\beta s)}{\sinh^2 a \cos^2(b+\beta s) + \sin^2(b+\beta s) \cosh^2 a}$$

$$\rho^2 = \frac{1}{|Z_1|^2} \left\{ A^2 + B^2 - (C^2+D^2) + \frac{(C^2+D^2)\cosh 2a + (AC+BD)\sinh 2a + (AD-BC)\sin 2(b+\beta s)}{\sinh^2 a + \sin^2(b+\beta s)} \right\}$$

(5.3)

This equation may be written

$$\rho^2 = K_1 + \frac{K_2 + K_3 \sin 2(b + \beta s)}{\sinh^2 a + \sin^2(b + \beta s)} \quad (3.4)$$

where K_1 , K_2 and K_3 are independent of s and are determined experimentally.

To simplify the experimental technique K_3 is made zero.

For this condition

$$AD - BC = 0$$

$$\begin{aligned} \text{i.e. } R_2^2 \sin \beta s_1 \cos \beta s_1 + X_2^2 \sin \beta s_1 \cos \beta s_1 - X_2 Z_0 \sin^2 \beta s_1 &= 0 \\ (Z_2^2 + Z_0 X_2 \tan \beta s_1) \sin \beta s_1 \cos \beta s_1 &= 0 \end{aligned}$$

The relevant solution of this equation is

$$\tan \beta s_1 = - \frac{Z_2^2}{Z_0 X_2}$$

This is the case of critical separation for which $S_1 = S_0$, say. With this condition fulfilled equation (3.4) becomes

$$\rho^2 = K_1 + \frac{K_2}{\sinh^2 a + \sin^2(b + \beta s)} \quad (3.5)$$

The determination of the constants a and b from this equation is described below. From a and b the value of Z may be calculated since

$$\frac{Z_0 - Z}{Z_0 + Z} = K = e^{-2r} = e^{-2(a + jb)}$$

Thus $Z = Z_0 \tanh(a + jb)$

Treating Z_0 as purely resistive the real or resistive component of Z , viz R , is given by

$$R = Z_0 \frac{\tanh a \sec^2 b}{1 + \tanh^2 a \tan^2 b} = Z_0 \frac{\sinh 2a}{\cosh 2a + \cos 2b} \quad (3.6)$$

Figure (3.2)

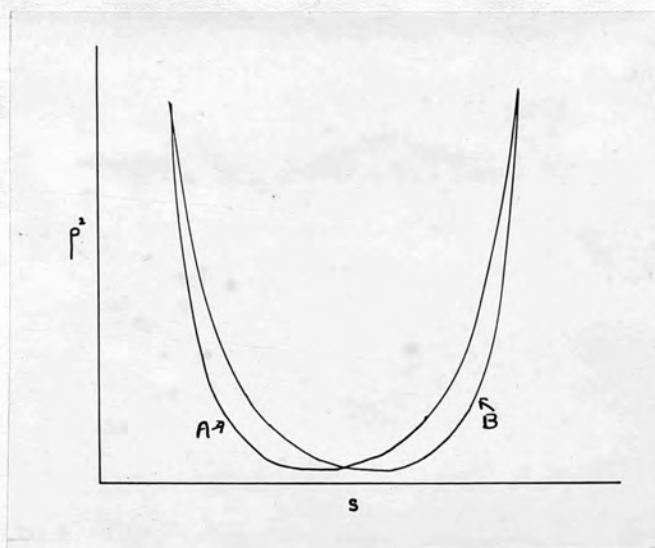
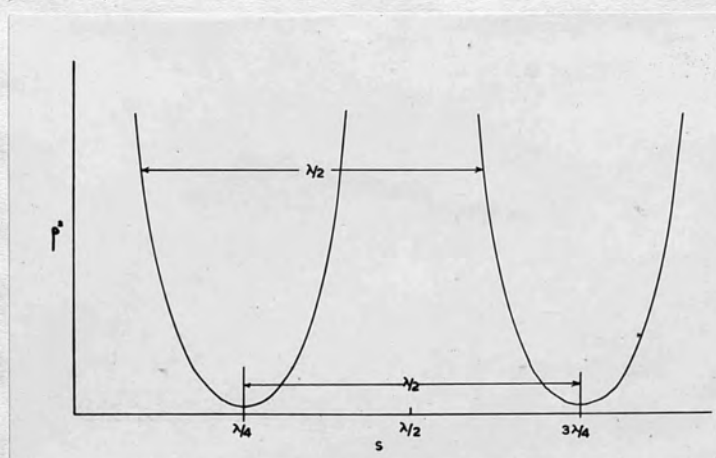


Figure (3.3)



and the unreal or reactive component, viz X, by

$$X = Z_0 \frac{\operatorname{sech}^2 a \cdot \tan b}{1 + \tanh^2 a \tan^2 b} = Z_0 \frac{\sin 2b}{\cosh 2a + \cos 2b} \quad (3.7)$$

In order to use equation (3.5) to determine the constants a and b it is first necessary to make $K_3 = 0$ in equation (3.4). To find the critical separation of the bridges which fulfils this condition the end of the line is shorted making $a = b = 0$ so that equation (3.4) becomes

$$\rho^2 = K_1 + K_2 \operatorname{cosec}^2 \beta s + 2K_3 \cot \beta s \quad (3.8)$$

From this equation it can be seen that a graph of ρ^2 against s is only symmetrical when $K_3 = 0$. This is the required position of critical separation when $S_1 = S_0$. If $S_1 > S_0$ the curve A of figure (3.2) is obtained and if $S_1 < S_0$ the curve B. In the critical position the first minimum value of ρ^2 occurs when $s = \frac{\lambda}{4}$ (figure 3.3). This position is found by adjusting the bridges until the value of ρ^2 at $s = \frac{\lambda}{4}$ is a minimum.

When the condition $S_1 = S_0$ (i.e. $K_3 = 0$) is satisfied equation (3.5) can be used instead of equation (3.4) and this is done for the remaining measurements. First K_1 is found by leaving the end of the line shorted ($a = b = 0$) and plotting a graph of ρ^2 against $\operatorname{cosec}^2 \beta s$. In this case equation (3.5) becomes

$$\rho^2 = K_1 + K_2 \operatorname{cosec}^2 \beta s$$

so that the graph is a straight line with intercept K_1 on the ρ^2 axis. The linearity of the graph is a criterion of the

nearness of the separation of the bridges to the critical value.

The short circuit at the end of the line is then replaced by the unknown impedance and a second ρ^2/S curve plotted with $S_1 = S_0$. It can be seen from equation (3.5) that the curve is symmetrical about the turning points so that these can be found accurately by drawing lines parallel to the s-axis.

The maxima of ρ^2 occur when

$$\sin^2(b + \beta s) = 0 \quad ; \quad b + \frac{2n\pi}{\lambda} s = n\pi \quad (3.9)$$

and the minima when

$$\sin^2(b + \beta s) = 1 \quad ; \quad b + \frac{2(n + \frac{1}{2})\pi}{\lambda} s = (n + \frac{1}{2})\pi \quad (3.10)$$

Thus the wavelength λ can be found from the distance between successive maxima and minima and, knowing λ , a value of b can be calculated from the position of each turning point using equations (3.9) and (3.10).

Equation (3.5) may be re-written

$$\frac{K_2}{\rho^2 - K_1} = \sinh^2 a + \sin^2(b + \beta s)$$

A graph of $\frac{1}{\rho^2 - K_1}$ plotted against $\sin^2(b + \beta s)$ is therefore linear (subject, of course, to the condition that the correct critical separation has been used) and has an intercept $\sinh^2 a$ on the $\sin^2(b + \beta s)$ axis. This is used to find a. Z_0 is usually calculated so that everything in equations (3.6) and (3.7) is known and R and X may be found.

Williams used this method to investigate the properties

of transformer oil. Most of the apparatus is the same as that described fully in Section IV(b) and will not be described here also. The Lecher wires were terminated in an air condenser and ρ^2/s curves were plotted firstly with the condenser surrounded by air and secondly immersed in the oil. Assuming a to be zero in each case, the two values of b were obtained directly from the turning points of the graphs. From equations (3.6) and (3.7) when $a = 0$, $R = 0$ and $X = Z_0 \tan b$. Thus if the values of b were b_1 and b_2 , respectively, the dielectric constant ϵ was given by

$$\epsilon = \frac{\tan b_1}{\tan b_2}$$

The method is quick and accurate for the measurement of impedances when the resistive component may be neglected.

b) THEORETICAL AND EXPERIMENTAL INVESTIGATION OF WILLIAMS' METHOD ((Miss) M. Williamson and (Miss) E. Harriss).

A critical experimental study of the double-bridge method was made by Miss E. Harriss and the results form her thesis for the M.Sc. degree of the University of London (1947).

In the first part of the work an alternative and more reliable method of finding the critical separation is suggested.

Williams account can be understood in two ways. It could mean that keeping S_1 fixed a graph of ρ^2 and s was plotted and the process repeated for different values of S_1 until the minimum value of ρ^2 occurred where $S = \frac{\lambda}{4}$. From equation (3.4) when $a = b = 0$ and $S_1 = S_0$ (i.e. $K_3 = 0$)

$$\rho^2 = K_1 + K_2 \operatorname{cosec}^2 \beta s \quad (3.11)$$

The ρ^2/S curve is thus symmetrical and by differentiating ρ^2 with respect to s the minimum of ρ^2 can be seen to occur at $S = \frac{\lambda}{4}$. This method therefore gives a correct value for the critical separation but is a trial and error one and may be long and tedious.

Alternatively Williams' statement may mean that s is kept fixed at $\frac{\lambda}{4}$ and one set of readings of S_1 and ρ^2 is taken, the minimum value of ρ^2 occurring when $S_1 = S_0$. It is shown by substituting $S = \frac{\lambda}{4}$ in equation (3.4) and differentiating ρ^2 with respect to S_1 that when ρ^2 is plotted against S_1 for $S = \frac{\lambda}{4}$ the minimum value of ρ^2 occurs at a value of S_1 which is not necessarily the critical separation. In fact it only

Figure ~~(3.4)~~ (3.5)

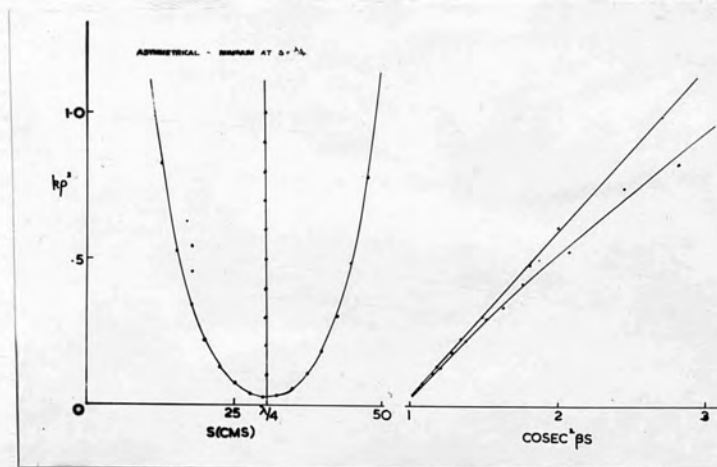
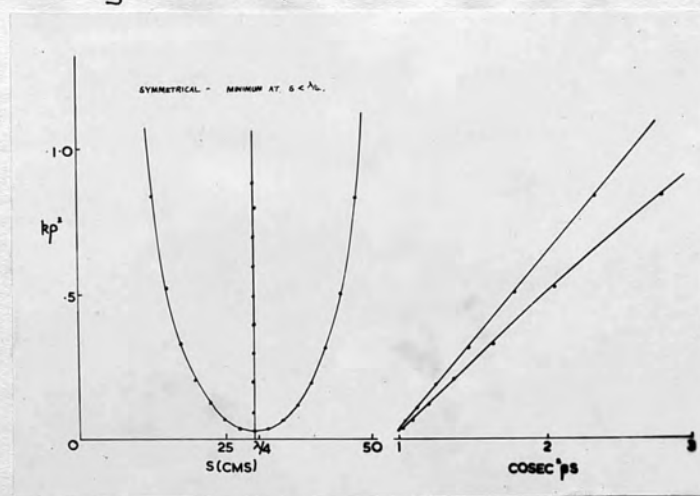


Figure ~~(3.5)~~ (3.4)



occurs at the critical separation when Z_2 is purely reactive.

After this analysis Miss Harriss suggests that to find the critical separation graphs of ρ^2 against s are plotted for various values of S_1 and the value of s for minimum ρ^2 found in each case. These values can then be used to find the critical separation directly. When $a = b = 0$ but $K_3 \neq 0$ equation (3.4) becomes

$$\rho^2 = K_1 + K_2 \operatorname{cosec}^2 \beta s + 2 K_3 \cot \beta s$$

By differentiating this equation with respect to s it is seen that at the minimum value of ρ^2

$$\cot \beta s_{\min} = - \frac{K_3}{K_2}$$

Substituting for K_3 and K_2 from equations (3.3) and (3.4)

$$\cot \beta s_{\min} = - \cot \beta s_1 - \frac{Z_0 X_2}{Z_2^2}$$

$$\therefore \cot \beta s_{\min} = - \cot \beta s_1 + \cot \beta s_0$$

So that if $\cot \beta s_{\min}$ is plotted against $\cot \beta s_1$, a straight line is obtained with an equal intercept $\cot \beta s_0$ on each axis from which S_0 can be calculated.

The results of an experimental investigation at a frequency of 250 Mc/s given in a further section of the thesis are in the form of a number of curves of ρ^2 plotted against s for various values of S_1 , with the corresponding graphs of ρ^2 against $\operatorname{cosec}^2 \beta s$. The ρ^2/s curves were not symmetrical when $S = \frac{\lambda}{4}$ as would appear from the theory. The corresponding $\rho^2/\operatorname{cosec}^2 \beta s$ graphs were not straight lines for the case when the ρ^2/s curves were symmetrical or when the minimum value

Figure (3.6)

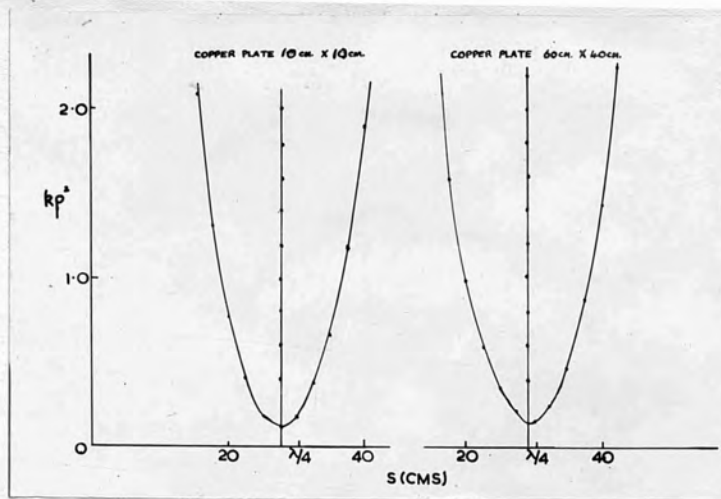


Figure (3.7)

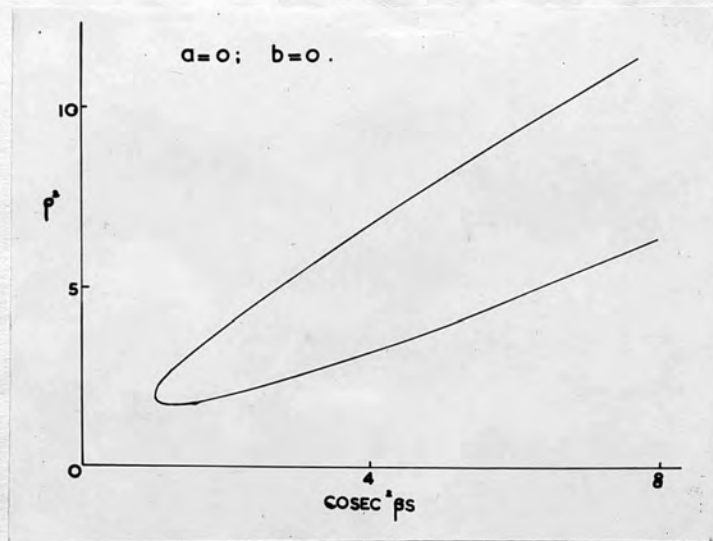
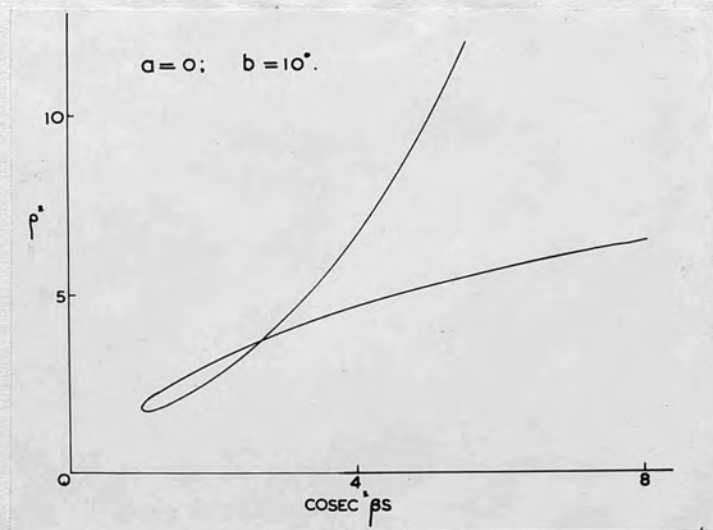


Figure (3.8)



of ρ^2 occurred at $S = \frac{\lambda}{4}$ (figures 3.4 and 3.5). It was concluded that these effects were due to the line being imperfectly shorted as a larger shorting-plate reduced the effect (figure 3.6).

Considering the original equation (3.4)

$$\rho^2 = K_1 + \frac{K_2 + K_3 \sin 2(b + \beta S)}{\sinh^2 \alpha + \sin^2(b + \beta S)}$$

it can be seen that whatever the values of a and b if

$K_3 = 0$ (i.e. $S_1 = S_0$) the ρ^2/S curve will be symmetrical.

However it is only when the ends are shorted ($a = b = 0$) in addition to the separation being critical ($K_3 = 0$) that equation (3.11) can be used and the minimum occurs when $S = \frac{\lambda}{4}$.

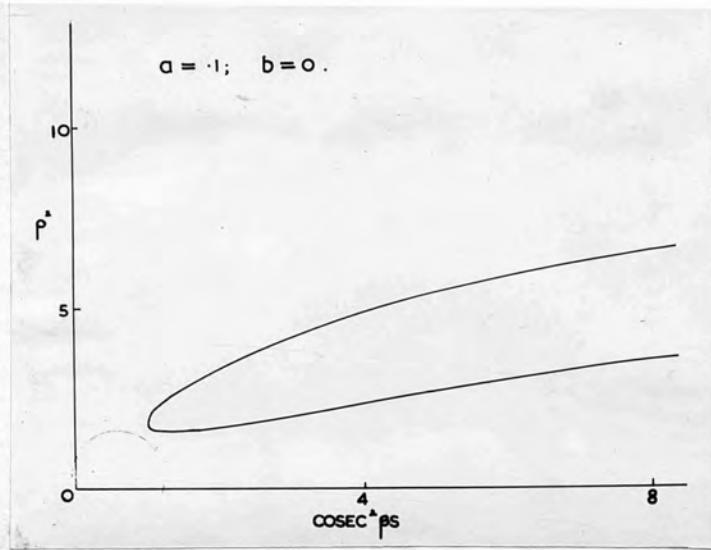
It can also be seen from equation (3.4) that it is only when these two conditions are fulfilled (i.e. $a = b = 0$ and $K_3 = 0$) that the $\rho^2/\text{cosec}^2 \beta S$ curve is a straight line.

The theory of this effect is discussed by Miss M. Williamson¹² in a recent paper in the Physical Society Proceedings. Theoretical graphs of ρ^2 against $\text{cosec}^2(b + \beta S)$ are shown with — finite values of a and b . When $a = 0$ and b is finite equation (3.4) becomes

$$\rho^2 = K_1 + K_2 \text{cosec}^2(b + \beta S) + 2K_3 \cot(b + \beta S)$$

The graph of ρ^2 against $\text{cosec}^2(b + \beta S)$ is the same as ρ^2 against $\text{cosec}^2 \beta S$ for the ideal case when $b = 0$ (figure 3.7) which becomes a straight line when $K_3 = 0$. However the graph of ρ^2 against $\text{cosec}^2 \beta S$ when $b \neq 0$ is of the form shown in figure (3.8). When a is finite and $b = 0$ equation (3.4) becomes

Figure (3.9)



Figure(3.10)

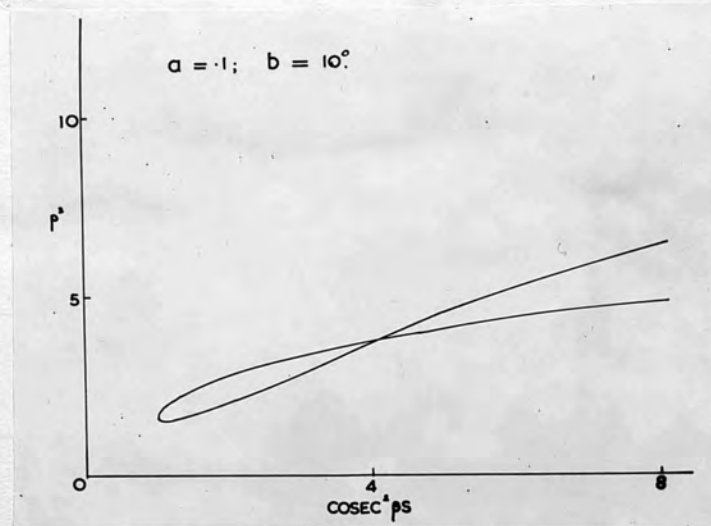
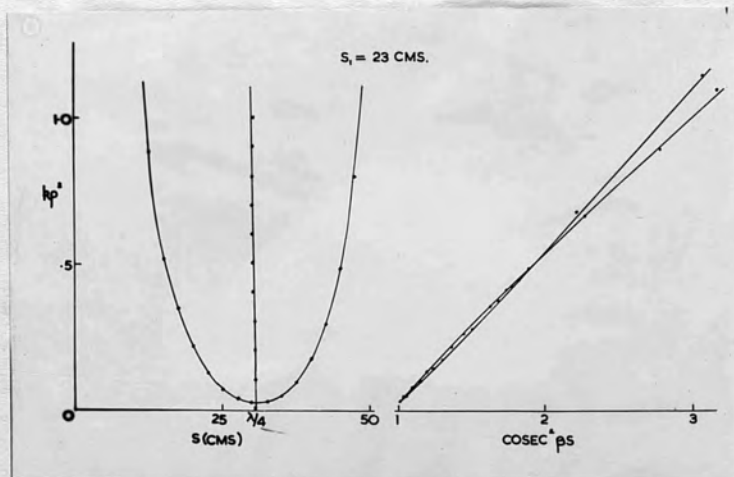


Figure (3.11)



$$\rho^2 = K_1 + \frac{K_2 \operatorname{cosec}^2 \beta S + 2 K_3 \sin \beta S \cos \beta S \operatorname{cosec}^2 \beta S}{\operatorname{cosec}^2 \beta S \sinh^2 a + 1}$$

$$\rho^2 (1 + \sinh^2 a \operatorname{cosec}^2 \beta S) = K_1 + K_1 (\sinh^2 a + K_2) \operatorname{cosec}^2 \beta S + 2 K_3 \cot \beta S$$

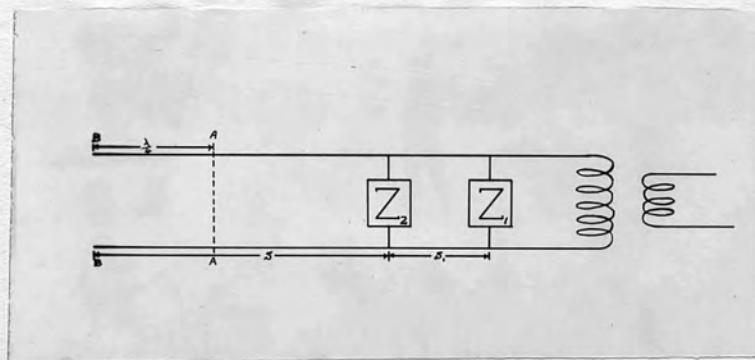
The factor multiplying ρ^2 imposes a downward curvature on both branches of the curve while that multiplying $\operatorname{cosec}^2 \beta S$ alters the slope of the whole graph. The shape of the curve is shown in figure (3.9). The two effects together are shown by the curve of figure (3.10) and figure (3.11) is an experimental curve for the purposes of comparison.

It is apparent from this investigation that although the correct critical separation and the value of b may be obtained from the graphs of an imperfectly shorted line it is essential to short the lines correctly in order to get a straight line graph of ρ^2 against $\operatorname{cosec}^2 \beta S$. It is from the intercept of this straight line that the value of K_1 and hence of a must be obtained.

SECTION IV

A NEW METHOD FOR FINDING THE CRITICAL
SEPARATION OF THE DOUBLE-BRIDGE METHOD

Figure (4.1)



a) THEORY OF THE METHOD

The necessity for perfect shorting of the line, mentioned in the last section, presents considerable mechanical difficulties in the case of open Lecher wires and the difficulty is likely to become greater at higher frequencies. Consequently it would seem worth while eliminating this necessity at the expense of making the experimental technique longer.

Consider equation (1.24) for the input impedance Z_i of a length of line l terminated in an impedance Z_T

$$Z_i = Z_0 \cdot \frac{Z_0 \sinh Pl + Z_T \cosh Pl}{Z_0 \cosh Pl + Z_T \sinh Pl}$$

If the end of the line is on open-circuit Z_T is infinitely great and the expression for Z_i becomes

$$Z_i = Z_0 \coth Pl$$

When $l = \frac{\lambda}{4}$, under these conditions, $Z_i = 0$.

Thus in figure (4.1) the part of the circuit to the left of AA may be effectively replaced by a short-circuit at AA.

To find the critical separation, instead of shorting the end of the line it may be left on open-circuit and is replaced by $(S - \frac{\lambda}{4})$ in the relevant equations. When S_1 has its critical value the curve of ρ^2 against s , with the line on open-circuit, should be symmetrical with its minimum occurring

$$\text{where } S - \frac{\lambda}{4} = \frac{\lambda}{4}$$

$$\text{i.e. } S = \frac{\lambda}{2}$$

Substituting $(s - \frac{\lambda}{4})$ for s as explained above, equation (3.11), which applies under the critical conditions and when the end of the line is shorted, becomes

$$\rho^2 = K_1 + K_2 \operatorname{cosec}^2 \beta (s - \frac{\lambda}{4})$$

A graph of ρ^2 against $\operatorname{cosec}^2 \beta (s - \frac{\lambda}{4})$ should, therefore, be a straight line with intercept K_1 .

After the critical separation and the constant K_1 have been found in this slightly different way the rest of the method is the same as before, the distances again being measured from the end of the line.

Figure (4.2)

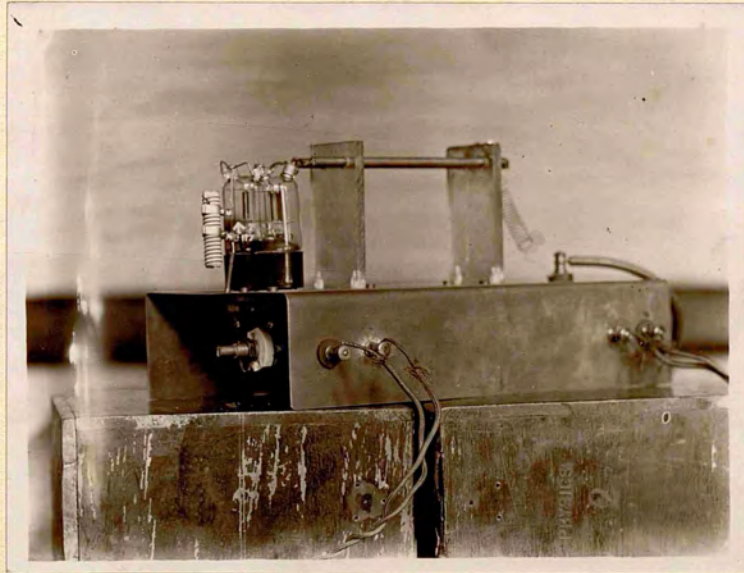
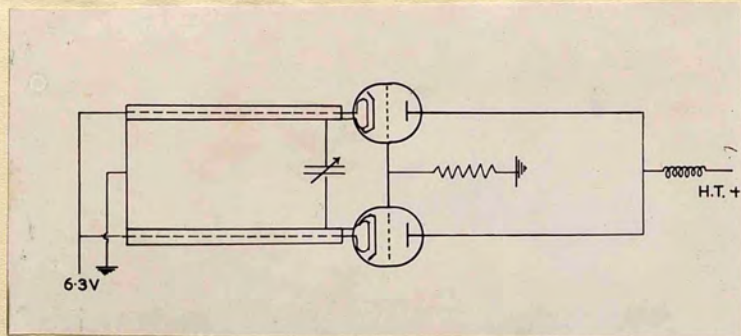


Figure (4.3)



b) EXPERIMENTAL WORK

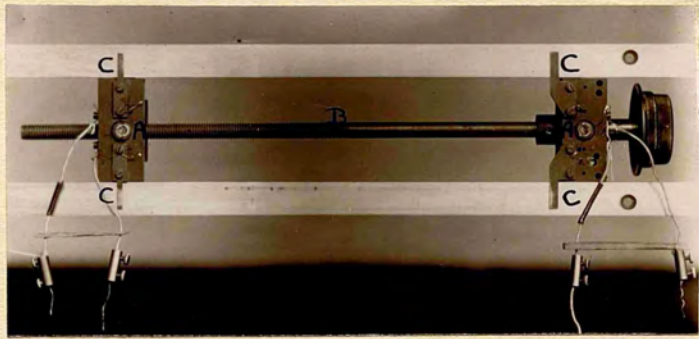
Experimental work was carried out to investigate whether the shorting of the lines could be dispensed with as described in the previous sub-section.

DESCRIPTION OF APPARATUS

Much of the apparatus was the same as that used by Dr. Williams and Miss Harriss. The transmission lines were of right-angle brass, three metres long and six centimetres apart and were supported by ebonite pillars. The characteristic impedance was taken as 191 ohms since that was the value used for the same lines by Dr. Williams and Miss Harriss. For the experimental work in this section one end of the lines was left on open-circuit and the oscillator was coupled to the other end by means of a loop of thick copper wire. The tightness of the coupling could be adjusted to obtain currents of a suitable value in Z_1 and Z_2 .

The oscillator and its circuit-diagram are shown in figures (4.2) and (4.3). The circuit was of the tuned-anode, tuned-cathode type with two indirectly heated triodes (E.1171) in push-pull. The tuned-cathode circuit consisted of a variable condenser across two coaxial lines and the tuned-anode circuit of two brass rods (together with the inter-valve capacities). It was the latter pair of rods that were coupled to the line. The oscillator was shielded by a metal case and power (6.3 volts for the heaters and 250 volts H.T.) was

Figure (4.4)



supplied by a mains stabilized power pack.

The impedances Z_1 and Z_2 are shown in position in figure (4.4). They were vacuum thermo-junctions (A) mounted in ebonite blocks connected by a rod of insulating material (B). The distance between the two bridges was adjusted by a screw thread on the rod. Brass knife edges (C) were screwed on to the blocks and made sliding contact with the lines. They were connected to the heater wires of the thermo-junction. The thermo-couple wires were connected to sensitive micro-ammeters via screws in the blocks.

At a given frequency the extra resistance of the heater wires due to the skin effect is constant so that the heat produced in Z_1 and Z_2 is proportional to \bar{I}_1^2 and \bar{I}_2^2 respectively where \bar{I}_1 and \bar{I}_2 are the currents flowing in Z_1 and Z_2 . Both thermo-junctions had previously been found to possess square-law characteristics so that the micro-ammeter readings were taken to be proportional to \bar{I}_1^2 and \bar{I}_2^2 . The ratio $\frac{\bar{I}_1^2}{\bar{I}_2^2}$ gave the value of $K\rho^2$ and it was not necessary to determine the constant K as the position of the minimum value of ρ^2 was all that was required.

The flex connecting the micro-ammeters to the thermo-couples was kept at right-angles to the lines to prevent stray fields being picked up from the currents flowing in the lines. The readings were taken with the observer at least a metre from the lines and always in the same position to avoid varying

Figure (4.5)

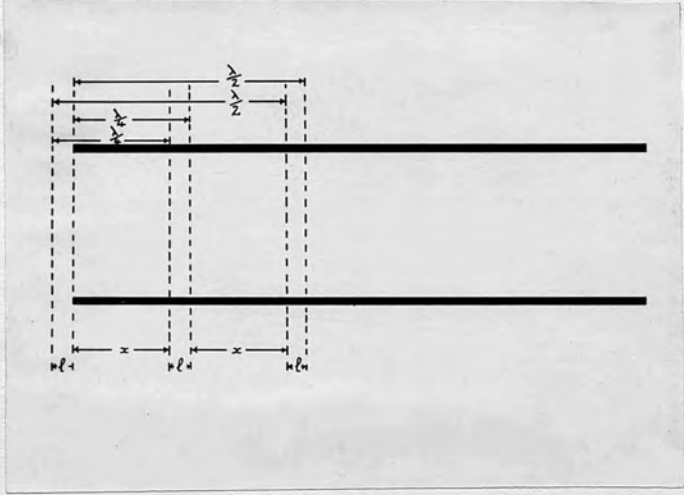
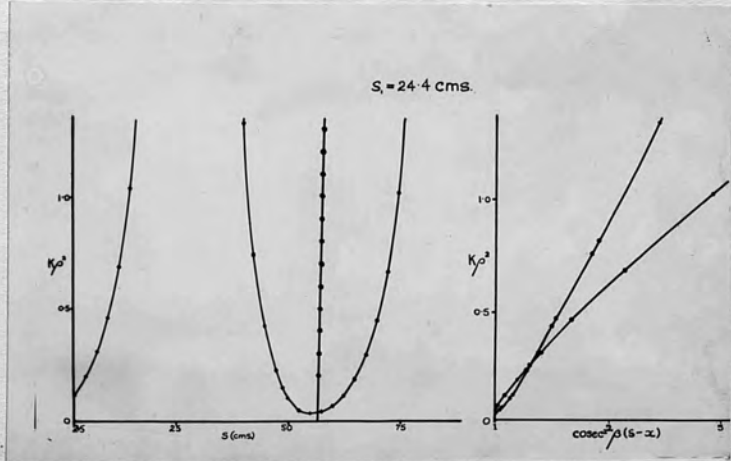


Figure (4.6)



capacitative effects.

RESULTS

When plotting experimental values of ρ^2 against s it was found that the minimum value of ρ^2 always occurred at a distance slightly less than $\frac{\lambda}{2}$ from the end of the line. Thus the open-circuit end-effect is equivalent to an extra length of line l where $l = \frac{\lambda}{2} -$ (distance of first minimum from the end of the line). This was allowed for by subtracting l from $\frac{\lambda}{4}$ to give a length x , say. Then the effective short-circuit at AA (see figure 4.1) is at a distance x from the end BB instead of a distance $\frac{\lambda}{4}$. This point is illustrated in figure (4.5). ρ^2 was therefore plotted against $\text{cosec}^2 \beta (s-x)$. It was found that the linearity of this latter graph was a much more sensitive test of the critical condition than the symmetry of the ρ^2/S curve.

Graphs of ρ^2/S and $\rho^2/\text{cosec}^2 \beta (s-x)$ were plotted for different values of S_1 . These are shown in figures (4.6), (4.7) and (4.8). In each case the end-effect l was 3.4 cm. The ρ^2/S curve appeared symmetrical both for $S_1 = 24.3$ cm (figure 4.7) and for $S_1 = 24.2$ cm (figure 4.8). However while the graph of $\rho^2/\text{cosec}^2 \beta (s-x)$ for $S_1 = 24.3$ cm (figure 4.7) approximated closely to a straight line a slight curvature was detectable at the lower end. The points on the $\rho^2/\text{cosec}^2 \beta (s-x)$ graph for $S_1 = 24.2$ cm (figure 4.8) lay very near to a straight

Figure (4.7)

Fig. [4.7(a)]

Fig. [4.7(b)]

$S_1 = 24.3 \text{ cms.}$

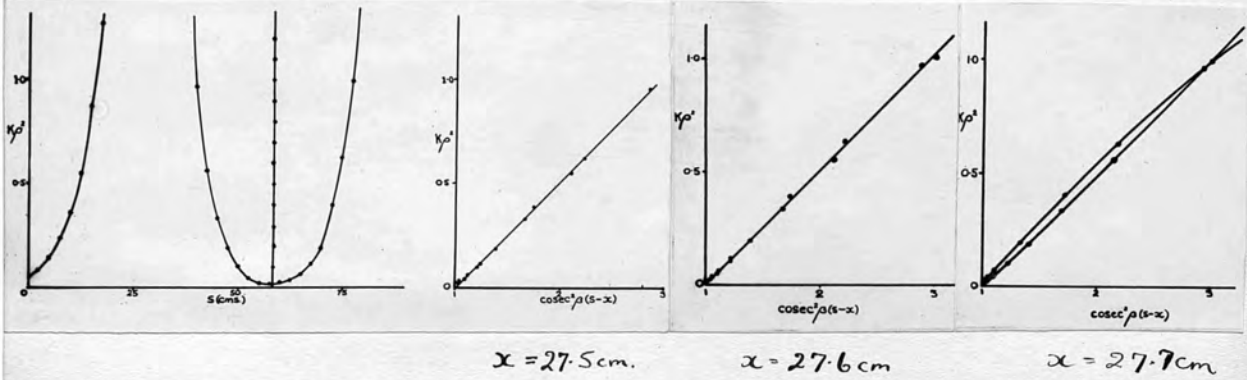
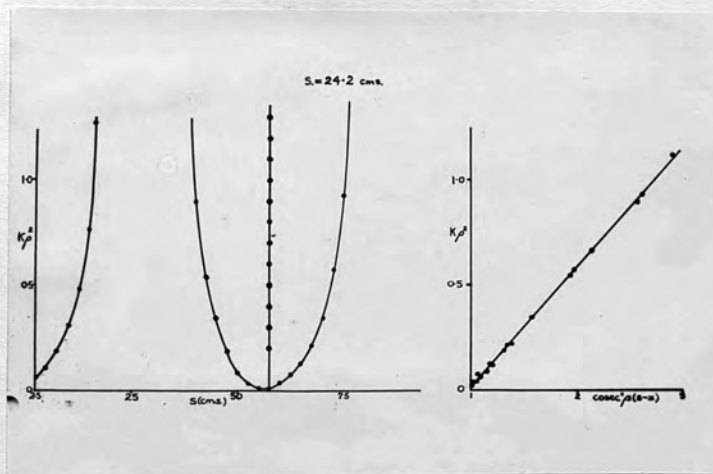


Figure (4.8)



line and so this value of S_1 was taken as the critical separation.

The intercepts K_1 on the ρ^2 axis were - 0.51 and - 0.53, respectively, so that although the latter was taken as correct the difference would not have had an appreciable effect when plotting the graph of $\frac{1}{\rho^2 - K_1}$ against $\sin^2(b + \beta s)$ to obtain a.

A further point which was investigated was the effect of a slight error in determining the end-effect l of the lines. For the first set of readings S_1 was 24.3 cm and the ρ^2/S graph is shown in figure (4.7). The first minimum of ρ^2 occurred at a distance of 58.5 cm from the end of the line as nearly as could be determined from the curve. The mean value of $\frac{\lambda}{2}$ from the graph was 61.94 cm so that the end-effect l was 3.44 cm. x (the distance of the effective short from the end of the lines) then equals $(\frac{\lambda}{4} - l)$ i.e. 27.53 cm. Since s can only be determined to the nearest millimetre graphs of $\rho^2/\text{cosec}^2\beta(s-x)$ were plotted for $x = 27.5$ cm, 27.6 cm and 27.7 cm (figures ~~4.9~~, ~~4.10~~ and ~~4.11~~).

For the first two of these graphs ($x = 27.5$ cm and $x = 27.6$ cm) the points lie very close to a straight line but when $x = 27.7$ cm two branches of the graph are noticeable and the curve is similar to the theoretical one when a and b are both finite (c.f. figure 3.10). The intercepts on the ρ^2 axis in each case were - 0.51, - 0.50 and - 0.49 respectively so

that the value obtained for K_1 is not appreciably affected by changes of one or two millimetres in the value of x . However the linearity of the $\rho^2/\text{cosec}^2\beta(s-x)$ curve does appear to be affected by a change of only a millimetre.

The experimental procedure for finding the critical separation and the value of K_1 now involves the following steps. First the bridges are set an arbitrary distance apart with the lines on open-circuit at one end. A set of readings of I_1^2 , I_2^2 and s is taken and a graph of ρ^2/s plotted. If the curve is obviously unsymmetrical there is nothing to be gained by plotting the $\rho^2/\text{cosec}^2\beta(s-x)$ graph. Further sets of readings are then taken for different values of S_1 until the ρ^2/s curve appears to be symmetrical. This should not be a long procedure as the direction of the slope of the ρ^2/s curves shows whether S_1 is too large or too small.

When the condition of symmetry is fulfilled the readings are used to plot a graph of ρ^2 against $\text{cosec}^2\beta(s-x)$. Although the ρ^2/s curve may appear symmetrical the $\rho^2/\text{cosec}^2\beta(s-x)$ graph may not be linear as the value of S_1 is much more critical for this condition. More ρ^2/s graphs with the corresponding $\rho^2/\text{cosec}^2\beta(s-x)$ graphs must then be plotted until the latter is linear. The value of S_1 corresponding to the linear $\rho^2/\text{cosec}^2\beta(s-x)$ graph is then the critical separation S_0 .

One difficulty that arises here is that when a $\rho^2/\text{cosec}^2\beta(s-x)$ graph is non-linear it may not be possible to tell whether the curvature is due to the value of S_1 not being the critical one

or the effective short-circuit being taken in the wrong place. The shape of the graph is sensitive to both of these factors and it may be difficult to separate them.

Unfortunately the whole experimental procedure to find the critical separation S_0 and the constant K_1 may be a lengthy and tedious process but if the same apparatus and frequency are used for the measurement of several impedances S_0 and K_1 need only be found once.

SECTION V.

THE MEASUREMENT OF AN IMPEDANCE USING
A SYSTEM OF LECHER WIRES.

In order to compare the two line methods of measuring impedance outlined in Sections II and III the apparatus described in Section IV(b) was used. The impedance of an air condenser was measured firstly by the Williams or double-bridge method (sub-section (a)) and secondly by the Chipman or current resonance method (sub-section (b)). In an attempt to eliminate the end-effects, which include the impedance of the leads to the condenser and of the joins at either end of the leads, readings were taken for two different values of the setting of the condenser.

a) RESULTS USING THE DOUBLE-BRIDGE METHOD.

From the experimental results recorded in the previous section it was concluded that the critical separation S_c between the bridges was 24.2 cms and that the value of K_1 was - 0.530.

An air-condenser set at an arbitrary dial reading (20) was connected across the open end of the line and keeping the distance between the bridges at 24.2 cms a further set of values of I_1^2 , I_2^2 and s were taken. A graph of ρ^2 against s was plotted as before (figure 5.1). From the positions of the maxima of this curve the value of b was calculated. (The maxima were obtained from the mean abscissae and were used in preference to the minima as their positions were less sensitive to the critical separation). The two values obtained for b ($+ 60.7^\circ$ and $+ 58.6^\circ$) were averaged giving $+ 59.6$.

The values of $\frac{1}{\rho^2 - K_1}$ and of $\sin^2(bt + \beta s)$ were then worked out for each value of s and the two plotted against each other (figure 5.2). The resultant graph has a very small intercept from which $\sinh^2 a$ was read and hence a found. The latter had a value of 0.186.

The dial setting of the air condenser was then moved to a second arbitrary value (80) and the measurements repeated. The ρ^2/s and $\frac{1}{\rho^2 - K_1} / \sin^2(bt + \beta s)$ graphs were similar in shape to figures (5.1) and (5.2) and have not been reproduced.

The value obtained for b in this case was $+ 67.3^{\circ}$ (mean of $+68.2^{\circ}$ and $+66.4^{\circ}$) and that for a 0.172 .

b) RESULTS USING THE CURRENT RESONANCE METHOD.

The equations in Chipman's paper are obtained in terms of the reflection coefficients K_T and K_G . It is easier to compare the results with those of Williams' method if they are in the same form, i.e. if they give a value for the same constants a and b from which the impedance Z is calculated by the equation

$$Z = Z_0 \tanh (a + jb) \quad (5.1)$$

The results of Chipman's method are given in the form of current reflection coefficients K_G and K_T where the suffixes G and T refer to the unknown impedance and the current measuring instrument respectively. From equation (1.4) the product $K_G K_T$ is given by

$$K_G K_T = e^{-2(p+jq)}$$

Since $K_T = \frac{Z_0 - Z_T}{Z_0 + Z_T}$ and $K_G = \frac{Z_0 - Z_G}{Z_0 + Z_G}$ by definition

$$\frac{Z_0 - Z_T}{Z_0 + Z_T} \cdot \frac{Z_0 - Z_G}{Z_0 + Z_G} = e^{-2(p+jq)} \quad (5.2)$$

Putting $Z_G = Z_0 \tanh (a_G + jb_G)$ and $Z_T = Z_0 \tanh (a_T + jb_T)$ } from (5.1)

and substituting in (5.2)

$$e^{-2[a_T + a_G + j(b_T + b_G)]} = e^{-2(p+jq)}$$

hence $\begin{cases} p = a_T + a_G & (5.3) \\ q = b_T + b_G & (5.4) \end{cases}$

The equation which applies when the unknown impedance Z_G is connected to the input end is equation (1.10), viz

$$\sinh^2 (\Delta l_0 + p) + \sin^2 \frac{2\pi}{\lambda} \cdot \Delta l = \{ \sinh^2 (\Delta l_0 + p) \} g^2$$

Putting $g = 2$ and substituting from equation (5.3)

$$\sinh (\Delta l_0 + a_T + a_G) = \sin \frac{\pi}{\lambda} \cdot \Delta l, \quad (5.5)$$

When the input end is shorted ($a_G = b_G = 0$) this becomes

$$\sinh(\alpha l_{s.c.} + a_T) = \sin \frac{\pi}{\lambda} \cdot \Delta l_{s.c.} \quad (5.6)$$

From equations (5.5) and (5.6)

$$\alpha_G = \sinh^{-1} \left\{ \sin \frac{\pi}{\lambda} \cdot \Delta l_1 \right\} - \sinh^{-1} \left\{ \sin \frac{\pi}{\lambda} \Delta l_{s.c.} \right\} - \alpha (l_0 - l_{s.c.}) \quad (5.7)$$

where l_0 and $l_{s.c.}$ are the resonant lengths when the power is injected through the unknown impedance or the shorting-plate and Δl_1 and $\Delta l_{s.c.}$ are the widths of the corresponding resonance curves at half their height.

From equations (1.7) and (1.12)

$$\begin{aligned} \phi_G &= \frac{4\pi}{\lambda} [l_0 - l_{s.c.}] \\ \phi_G &= \phi_{TG} - \phi_T \\ &= -2(b_G + b_T - b_T) \\ &= -2b_G \\ \therefore b_G &= \frac{2\pi}{\lambda} [l_{s.c.} - l_0] \quad (5.8) \end{aligned}$$

The apparatus used to investigate Williams' method was suitable for the current resonance measurements with very little adaptation. In this case the power input to the line was first through a shorting-plate and then through the impedance to be measured. The current measuring instrument was one of the vacuum thermo-junctions used in Williams' method mounted and connected as before, i.e. the heater resistance was connected to knife edges which moved along the lines and the thermo-couple leads were connected to a sensitive micro-ammeter. The second thermo-junction was replaced by a reflecting plate (27 x 17 cm) of polished copper and the distance between the two was kept

Figure (5.3)

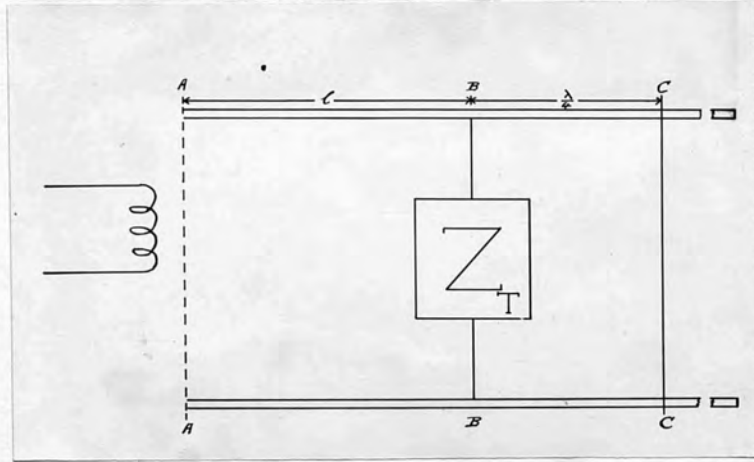


Figure (5.4)

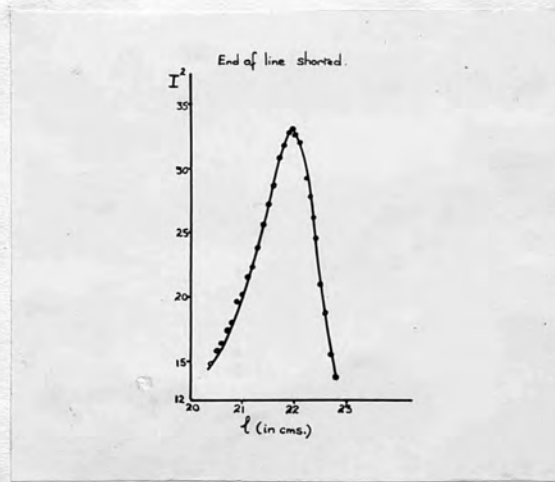


Figure (5.5)

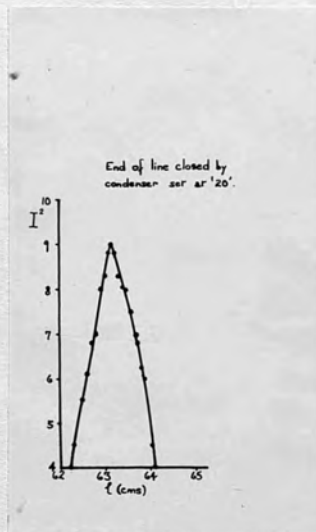
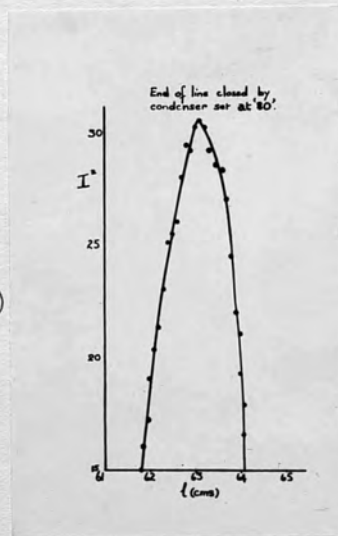


Figure (5.6)



fixed at $\frac{\lambda}{4}$ (figure 5.3).

For the first set of readings a polished copper plate (10 x 10 cm) was screwed on to the lines at AA and the current in the micro-ammeter, connected to the thermo-couple leads of the thermo-junction, was read for different values of l near the point of resonance. The readings were proportional to the square of the current flowing in the heater wire and were plotted against l to give the graph of figure (5.4). The resonant length of line $l_{s.c.}$ and the width of the curve at half its height $\Delta l_{s.c.}$ were read off the graph.

The shorting-plate was then replaced by the air condenser with the dial set at the same two readings as in the experimental work on Williams' method. In each case readings of I^2 and l were taken, resonance curves plotted (figures 5.5 and 5.6) and the values of l_1 and Δl_1 found as before. These values were substituted in equations (5.7) and (5.8). For the two settings of the condenser a was 0.065 and 0.025 and b was 56.4° and 56.6°

c) COMPARISON AND DISCUSSION OF RESULTS.

The tabulated results for the two methods are shown below

	Williams' method	Chipman's method
Condenser at dial reading 20.	$a = 0.186$ $b = +59.6^\circ$	$a = 0.065$ $b = +56.4^\circ$
Condenser at dial reading 80.	$a = 0.172$ $b = +67.3^\circ$	$a = 0.025$ $b = +56.6^\circ$

The values obtained for a by the two methods are quite inconsistent and those for b do not agree at all closely. The probable sources of error can be divided into three groups namely those common to both methods and those particular to one method only.

In the first group there is firstly the fact that the air condenser is not a balanced load. Secondly the general inaccuracies inherent in the use of open lines also apply to both methods. Among these are the effects of stray fields, the capacitative effect of nearby objects and the difficulty of shorting the lines adequately. This latter point has already been discussed fully with reference to Williams' method and it applies equally, of course, to Chipman's method. Thirdly the exact point of contact of the knife edges could not be determined within one or two millimetres.

The other main source of error in Williams' method is the fact that a is determined from the intercept of the $\frac{1}{\rho^2 - K_1} / \sin^2(\theta/\beta s)$

graph and this intercept is very small and therefore difficult to measure accurately.

When taking readings during the experimental work on Chipman's method the effects of random voltage fluctuations were very noticeable although the power pack was mains stabilized. The only way to minimize these effects was to take the readings near the point of resonance as quickly as possible. The fluctuations affect the value obtained for the resonant half-width of the curve to a much greater extent than the position of resonance. Thus it is the value of a rather than b that is inaccurate for this reason. In fact both this effect and the one mentioned in the previous paragraph affect the measurement of a and not of b .

CONCLUSION

It appears from the discussion in the last section that most of the sources of error in the experimental work on Williams' method would not occur if a closed line were used instead of the Lecher wire system. A closed line eliminates the capacitative effect of nearby objects and of stray fields. Also it is possible according to Essen's work (page 41) to short the line with negligible error. This would enable the critical separation and the constant K_1 to be found without lengthening the experimental procedure as suggested in Section IV. The most suitable method, when the end of the line can be correctly shorted, appears to be the direct one suggested by Miss Harriss in Section III(b) (page 54).

The screened twin or coaxial type of line described in Essen's work (figures 2.5 and 2.6) would be suitable according to whether the load was balanced or unbalanced. Some preliminary experimental work on Williams' method has been started using a coaxial line but it has not progressed far enough to justify an account. The micro-ammeter readings appear very steady, despite any external fields, and the ρ^2/s curves are much smoother than those obtained with open Lecher wires and are easily repeated.

If the investigation were to prove successful it might be possible to find the value of a for liquid dielectrics by introducing the liquid into the end of the coaxial line in an

upright position. This quantity α is the important one in the case of dielectrics which show absorption.

REFERENCES

1. R.A. Chipman Journal of Applied Physics 1939,
10, p.27.
2. Willis Jackson High Frequency Transmission Lines
p.62, equation (4.6).
3. H. Kaufmann Hochfrequenztechnik und
Elektroakustik 1939, 53, p.61.
4. Miller and Salzberg R.C.A. Review 1939, 3, p.486.
5. H. Brückmann Hochfrequenztechnik und
Elektroakustik 1938, 51, p.128.
6. H.T. Flint and G. Williams. Philosophical Magazine 1941, 32,
p. 489.
7. D. Rogers Proceedings of the Physical Society
1944, 56, p.1.
8. D. Rogers and G. Williams. Nature 1942, 149, p.668.
9. G. Williams Proceedings of the Physical Society
1944, 56, p.63.
10. Jackson and Huxley I.E.E. 1944, 91, Part III, p.105.
11. L. Essen I.E.E., 1944, 91, Part III, p.84.
12. (Miss) M. Williamson Proceedings of the Physical Society
1948, 60, p.388.